Research Paper

Clinical significance, tumor immune landscape and immunotherapy responses of ADAR in pan-cancer and its association with proliferation and metastasis of bladder cancer

Hao Yu[1,2,*], Kexin Bai[1,2,*], Yidong Cheng[1,*], Jiancheng Lv[1,2,*], Qiang Song[1], Haiwei Yang[1,2], Qiang Lu[1], Xiao Yang[1]

[1]Department of Urology, The First Affiliated Hospital of Nanjing Medical University, Nanjing 210029, PR China
[2]Institute of Urology and Andrology, Nanjing Medical University, Nanjing 210029, PR China
[*]Equal contribution

Correspondence to: Xiao Yang, Qiang Lu, Haiwei Yang; **email:** yangxiao2915@163.com, https://orcid.org/0000-0002-5429-9162; doctorlvqiang@njmu.edu.cn, haiweiyang@njmu.edu.cn
Keywords: ADAR, cancer, immunotherapy, bladder cancer, tumor immune microenvironment
Received: April 21, 2023 **Accepted:** June 19, 2023 **Published:** July 6, 2023

ABSTRACT

Background: ADAR is an enzyme involved in adenosine-inosine RNA editing. However, the role of ADAR in tumorigenesis, progression, and immunotherapy has not been fully elucidated.

Methods: The TCGA, GTEx and GEO databases were extensively utilized to explore the expression level of ADAR across cancers. Combined with the clinical information of patients, the risk profile of ADAR in various cancers was delineated. We identified pathways enriched in ADAR and their related genes and explored the association between ADAR expression and the cancer immune microenvironment score and response to immunotherapy. Finally, we specifically explored the potential value of ADAR in the treatment of the bladder cancer immune response and verified the critical role of ADAR in the development and progression of bladder cancer through experiments.

Results: ADAR is highly expressed in most cancers at both the RNA and protein level. ADAR is associated with the aggressiveness of some cancers, especially bladder cancer. In addition, ADAR is associated with immune-related genes, especially immune checkpoint genes, in the tumor immune microenvironment. Moreover, ADAR expression is positively correlated with tumor mutation burden and microsatellite instability in a variety of cancers, indicating that ADAR could be used as a biomarker of immunotherapy. Finally, we demonstrated that ADAR is a key pathogenic factor in bladder cancer. ADAR promoted proliferation and metastasis of bladder cancer cells.

Conclusion: ADAR regulates the tumor immune microenvironment and can be used as a biomarker of the tumor immunotherapy response, providing a novel strategy for the treatment of tumors, especially bladder cancer.

INTRODUCTION

After decades of unremitting efforts by medical scientists, great progress has been made in cancer treatment strategies and clinical outcomes. However, many patients remain stranded in the shadow of drug resistance, disease progression, relapse, and eventual death [1]. Among a variety of treatment modalities, antitumor immunotherapy has received sufficient attention in recent years and has achieved considerable

survival benefits in the treatment of multiple cancers, such as breast cancer, melanoma, lung cancer and colorectal cancer [2–5]. Common antitumor immunotherapy methods include therapeutic monoclonal antibody immunotherapy, immune checkpoint inhibitor (ICI) therapy, adoptive cell therapy, oncolytic virus therapy, and tumor vaccines [6, 7]. Among them, the development of immune checkpoint inhibitors represented by PD-1 inhibitors has attracted particular attention. Since only a minority of patients respond to ICIs, the identification of predictive markers and mechanisms of immunotherapy resistance are the subject of intensive research [6, 8]. Therefore, it is necessary to continuously improve the understanding of the pathogenesis of cancer and constantly improve the exploration of the characteristics of tumor genomics and the immune microenvironment to predict and improve the specificity and sensitivity of ICIs to tumor patients and reduce their toxic effects.

As a highly conserved group of enzymes, the adenosine deaminase acting on RNA (ADAR) family mediates adenosine to inosine (A-to-I) RNA editing, by which adenosines are selectively converted to inosines in double-stranded RNA (dsRNA) substrates [9]. However, the overall biological effects of ADAR remain largely unknown. There are three types of ADAR, ADAR1-3, in mammalian cells. Among them, ADAR1 was the first identified ADAR protein and has been extensively studied [10, 11]. Studies have shown that the abnormal expression and dysfunction of ADAR1 may have oncogenic or tumor suppressive effects, affecting tumor proliferation, invasion and response to immunotherapy [12]. For example, early-stage lung cancer patients with ADAR1 amplification often suffer a poor prognosis [13]. In addition, the abnormal upregulation of ADAR1 can promote the proliferation of triple-negative breast cancer cells [14]. Although the functions of ADAR in human cancers have been intensively studied, the specific roles and molecular mechanisms of ADAR in the tumor microenvironment and antitumor immunotherapy remain largely enigmatic.

Given the significance of ADAR, we performed comprehensive bioinformatics analysis and *in vitro* experiments to explore the important role and special molecular mechanisms of ADAR across cancers. First, by integrating information from multiple databases, we found that ADAR is abnormally upregulated in most cancers, including at the transcriptional and protein levels, and is associated with the malignancy and prognosis of a variety of cancers. Subsequently, we explored ADAR mutations, associated genes, and potential molecular pathways across cancers. Notably, we identified the relationship between ADAR and the tumor microenvironment (TME), ICIs, and their regulatory role in immune infiltration and immunotherapy. Finally, we independently investigated the role of ADAR in BLCA and its potential as an immunotherapeutic target, which was validated by a series of experiments. Our findings suggest that ADAR can be used as a biomarker to predict the prognosis of patients with BLCA.

MATERIALS AND METHODS

Data collection and processing

Pan-cancer sequencing data and clinicopathological information were downloaded from the TCGA (https://portal.gdc.cancer.gov/), GEO (https://www.ncbi.nlm.nih.gov/geo/), and GTEx databases (https://www.gtexportal.org/). To minimize batch effects, we used transcripts per million (TPM) and normalized them by log2 transformation on the same sequencing platform. The ADAR protein profiles were obtained from the UALCAN database (http://ualcan.path.uab.edu/). ADAR gene mutation data were obtained from the cBioPortal database (http://www.cbioportal.org/). Differences in ADAR mRNA expression between normal and tumor samples were analyzed using the "limma" R package among TCGA, GEO, and GTEx data. ADAR single-cell analysis was analyzed by using HPA. For two groups of *t*-tests, $p < 0.05$ indicated that the expression difference between tumor and normal tissues was statistically significant.

Relationship with histological grades, cox regression analysis, and survival analysis

Based on the mRNA sequencing data of ADAR in the TCGA database and the clinical information of patients, an independent sample *t*-test was used to analyze the expression difference of ADAR between different histological grades in pan-cancer. Cox regression analysis was used to investigate the relationship between ADAR expression and overall survival (OS), disease-specific survival (DSS), progression-free survival (PFS), and disease-free survival (DFS) in each cancer type. The "forest plot", "ggrisk", "survminer", "survival" and "timeROC" R packages were utilized to visualize the survival analysis. The log-rank test was used to compare differences in survival between these groups. TimeROC (v 0.4) analysis was used to compare the predictive accuracy of ADAR mRNA. For Kaplan-Meier curves, *p*-values and hazard ratios (HRs) with 95% confidence intervals (CIs) were generated by log-rank tests and univariate Cox proportional hazards regression. $P < 0.05$ was considered statistically significant.

Analysis of ADAR genomic alterations

The genomic mutational landscape of ADAR across cancers was obtained from the cBioPortal database, including alteration frequency, copy number alterations, and mutations. The mutation sites of ADAR are displayed through the schematic diagram or 3D (three-dimensional) structure of the "mutation" module.

Protein–protein interaction (PPI) network construction and functional enrichment analysis

Through the String database (https://string-db.org/), the top 50 genes that have been verified by experiments to interact with ADAR were obtained and displayed. Subsequently, we obtained the top 100 genes significantly associated with ADAR across cancers via the GEPIA 2 website (http://gepia2.cancer-pku.cn/#index). The key gene sets obtained from the two databases were intersected to obtain the optimal gene(s). In addition, we systematically analyzed the 5 genes with the highest correlation scores. Finally, Gene Ontology (GO), Kyoto Encyclopedia of Genes and Genomes (KEGG) and gene set enrichment analyses (GSEA) were performed to identify the molecular functions and pathways enriched in these genes. $P < 0.05$ was considered statistically significant.

Analysis of immune infiltration and immune-related genes

The ESTIMATE algorithm was used to explore the infiltration level of immune cells and stromal cells, and the stromal score and immune score were calculated. In addition, Spearman correlation analysis was used to generate correlation heatmaps showing the association between ADAR and immunomodulators (immune-stimulators, MHC genes, chemokines, and chemokine receptors) and immune checkpoint genes. The correlation between ADAR gene expression and tumor mutation burden/microsatellite instability (TMB/MSI) was analyzed by the Spearman method using the "ggstatsplot" R package.

Bioinformatics exploration of ADAR in BLCA

The TCGA-BLCA samples were divided into a high expression group and a low expression group according to the median value of ADAR expression. The "limma" package in R software was used to study the differentially expressed mRNAs. Adjusted $P < 0.05$ and |Log2 (Fold Change)| >1 were defined as the threshold for the differential expression of mRNAs. The mutation data were downloaded and visualized using the "maftools" package in R software. Oncoplot showed the differences between the somatic landscapes of the two cohorts of BLCA. To further confirm the underlying function of potential targets, the data were analyzed by functional enrichment (GO and KEGG).

We used the Timer 2.0 (http://timer.cistrome.org/) database to characterize the immune cell infiltration landscape in the 6 TCGA-BLCA samples with the highest (TCGA-FD-A3SR-01, TCGA−FD−A3SR−01, TCGA−GC−A3RB−01) and the lowest ADAR expression (TCGA-CF-A3MI-01, TCGA−CF−A47T−01, and TCGA−ZF−A9R4−01). Immunophenograms were constructed to visualize the immunophenotypes of samples in The Cancer Immunome Atlas (TCIA; https://www.tcia.at/home) database. The immunophenogram enables the calculation of an aggregated score, the immunophenoscore (IPS), based on the expression of major determinants, identified by a random forest approach. These factors were classified into four categories: MHC molecules (MHC), immunomodulators (CP), effector cells (EC), and suppressor cells (SC). The database notes that the IPSs were calculated on a 0-10 scale based on the expression of representative genes or gene sets of the immunophenogram. Sample z scores were positively weighted according to stimulator cell type and negatively weighted according to suppressor cell type and then averaged [15]. Subsequently, the IPS was also calculated for all patients in TCGA-BLCA, grouped according to ADAR expression. A potential immune checkpoint blockade (ICB) response was predicted with the Tumor Immune Dysfunction and Exclusion (TIDE) algorithm [16]. Two immunotherapy cohorts, IMvigor210 ($n = 348$) and GSE176307 ($n = 90$), were used to compare ADAR expression levels between groups with different responses to immune checkpoint blockades.

Clinical specimens

Bladder cancer tissues and their matched para-carcinoma tissues were taken from BLCA patients who underwent surgery at the First Affiliated Hospital of Nanjing Medical University from 2016 to 2019. The deadline for follow-up was June 2022. All patients signed the informed consent form before the use of clinical materials. The Ethics Committee of the First Affiliated Hospital of Nanjing Medical University approved the protocol used in this study.

RNA isolation and qRT PCR

Total RNA was extracted from bladder cancer tissues and cell lines using TRIzol reagent (Invitrogen, Thermo-Fisher Scientific, USA) according to the manufacturer's instructions. HiScript II (Vazyme,

China) was used to synthesize cDNA. qRT-PCR of mRNA was performed on a StepOne Plus real-time PCR system (Applied Biosystems, USA). Each sample was repeated three times, and the data were analyzed by comparing CT values. Primer sequences included ADAR: ′F: ATCAGCGGGCTGTTAGAATATG′ and ′R: AAACTCTCGGCCATTGATGAC′ and β-Actin: ′F: GGAGATTACTGCCTGGCTCCA′ and ′R: GACT CATCGTACTCCTGCTTGCTG′, purchased from TSINGKE Biological Technology (Beijing, China). We calculated multiple changes in mRNA expression by the $2^{-\Delta\Delta CT}$ method.

Western blot

Total tissue and cellular protein were dissolved in RIPA buffer (Sigma, USA) containing a protease inhibitor. The extracted proteins were quantified by bicinchoninic acid (BCA) analysis (Beyotime, China). The protein extracts were isolated by 10% SDS-PAGE and transferred to polyvinylidene fluoride (PVDF) membranes (Millipore, USA). High-affinity anti-ADAR1 antibodies (1:1000, Abcam, USA) and anti-β-actin antibodies (1:1000, Cell Signaling Technology, USA) were used. After incubation, the membrane was incubated with a secondary antibody (1:5000, Cell Signaling Technology, USA) conjugated with peroxidase (HRP). After cleaning, the signal was detected using a chemiluminescence system (Millipore, USA) and analyzed using Image Lab Software (Bio-Rad, USA).

Tissue microarray (TMA) and immunohistochemistry (IHC)

TMA was constructed from 180 bladder cancer tissues. Microwave heating was used to isolate the antigens. After dipping in 3% H_2O_2 for 10 min, the slides were treated with ADAR (1:200; Abcam, USA) at 4°C overnight. Afterward, HRP-conjugated antibody was used to treat the slides at room temperature for 30 min. Images were captured and recorded under a microscope (Nikon Corporation, Japan). Standard staining protocols were used. Stained tissues were scored for staining intensity (SI) and the percentage of positive cells (PP). SI was scored on a scale of 0–3 (0, negative staining; 1, weak staining; 2, moderate staining; 3, strong staining), and PP was scored according to five categories: 0 (0% positive cells), 1 (<10%), 2 (11–50%), 3 (51–80%) or 4 (>80% positive cells). The total score was calculated by multiplying the SI and PP scores, ranging from 0–12. Two pathologists who were blinded to the clinical parameters provided the respective scores. Different scores were divided into low-staining (0–7) and high-staining (8–12) groups.

Cell culture

BLCA cell lines (T24, BIU87, J82, 253J, 5637, RT4) and one human ureteral epithelial immortalized cell line (SV-HUC-1) were purchased from the Typical Culture Collection Center of the Chinese Academy of Sciences (Shanghai, China), and 10% fetal bovine serum (FBS; Biological Industries, Israel) and 1% penicillin/streptomycin (Gibco, Thermo Fisher Scientific, USA) were included in the study. All cell lines were cultured at 37°C in a humidified incubator containing 5% CO_2.

Transfection

Lentiviruses constructed for ADAR knockdown were obtained from OBiO Technology Corp., Ltd. (China). Cells were plated in 6-well dishes until 30% confluence was reached, infected with ADAR overexpression lentivirus (pcSLenti-EF1-EGFP-P2A-Puro-CMV-ADAR-3xFLAG-WPRE, termed as ADAR), a negative control (pcSLenti-EF1-EGFP-P2A-Puro-CMV-MCS-3xFLAG-WPRE, termed as NC); ADAR knockdown lentivirus (pSLenti-U6-shRNA(ADAR)-CMV-EGFP-F2A-Puro-WPRE, termed as shADAR-1 and shADAR-2), and scramble control (pSLenti-U6-shRNA(NC)-CMV-EGFP-F2A-Puro-WPRE, termed as shNC) in bladder cancer cell T24 and BIU87. Structures of stably transduced cells were generated by selection using puromycin (2.5 μg/ml) for 1 week.

Cell proliferation and colony formation assay

For the cell proliferation assay, cells were evenly spread in a 96-well plate at a density of 2000 cells/well. At 24, 48, 72 and 96 hours after inoculation, the cells were incubated in 10 μl/well CCK-8 diluted for 1 hour. The absorbance was measured at 450 nm with a microplate reader following incubation at 37°C for 1 h according to the manufacturer's instructions. For the colony formation assay, T24 and BIU87 cells were inoculated on 6-well plates at a rate of 1000 cells/well and incubated in 5% CO_2 at 37°C for 2 weeks. After fixation with methanol, the cells were stained with 0.1% crystal violet for 30 minutes, and then the colonies were imaged and counted.

Transwell cell invasion assay

Transfected cells were seeded into the upper chambers with serum-free medium coated with Matrigel (BD Biosciences, USA) for the invasion assay. Medium containing 20% FBS was added to the bottom chamber. After incubation for 24 h at 37°C, cells attached to the upper surface of the membrane were carefully removed with a cotton swab, and cells attached to the lower

surface of the membrane were fixed with 10% formalin, stained with crystal violet for 30 min at room temperature and counted.

Wound healing assay

To determine the effect of ADAR on cell migration, we uniformly inoculated transfected T24 and BIU87 cells in a 6-well plate. When the cell density reached 90-95%, a 200 μl pipette tip was used to draw a straight wound through the cell layer. The cells were washed with phosphate buffered saline (PBS) to remove the isolated cells and kept at 37°C in a humidified incubator containing 5% CO_2. A digital camera system (Olympus, Tokyo, Japan) was used to take images of wound closure at 0 and 24 hours.

Statistical analysis

The Wilcoxon rank-sum test was used to compare the differences between the two groups. The K-W test was performed to compare three or more groups. All statistical analyses were performed using R 4.1.0. Statistical significance was set at a two-sided *p*-value <0.05.

Data availability statement

The original contributions presented in the study are included in the article/Supplementary Materials. Further inquiries can be directed to the corresponding authors.

RESULTS

Upregulated expression of ADAR in cancers

We first illustrated the mRNA expression of ADAR in normal versus cancer tissues in pan-cancer using the TCGA database. The results showed that ADAR expression was upregulated in most cancers but downregulated only in GBM, KICH, and SKCM (Figure 1A). Since there were few normal samples included in the TCGA database, we added samples from the GTEx database and drew the expression of ADAR again. The results of our secondary analysis showed that the expression trend of ADAR was basically consistent with the results of the TCGA database, but there were some differences. For example, the expression of ADAR was upregulated in SKCM, THCA, and UCEC (Figure 1B). The results of paired difference analysis in the TCGA cohort showed that ADAR was generally highly expressed across cancers (Figure 1C). In addition, the UALCAN database was used to study the differences in ADAR protein levels between cancer and normal tissues in multiple cancers. Consistent with transcription levels, ADAR protein levels are significantly elevated in a variety of cancers (Figure 1D). Finally, to avoid bias in the analysis from a single database, we also collected independent datasets from multiple cancers in the GEO database. The results showed that ADAR expression was upregulated in most tumors except ACC, COAD, and PRAD, which was basically consistent with the analysis results from the TCGA database (Figure 1E).

Effect of ADAR on clinical manifestations and prognosis of pan-cancer

Recognizing that ADAR expression is upregulated in cancer, we further explored its potential role in cancer malignancy. A boxplot showed that ADAR expression was positively correlated with a higher pathological grade in BLCA, CESC, LIHC, UCEC, and PAAD, with the highest confidence in BLCA (AUC = 0.732) (Supplementary Figure 1).

Cox hazard regression forest plots showed that high ADAR expression was associated with poor OS in ACC (HR = 2.73053, $P = 0.0123$), KIRP (HR = 8.65333, $P = 0.0420$), and LGG (HR = 1.85562, $P = 0.0014$) (Supplementary Figure 2A). Risk profiles and survival analyses confirm this conclusion. High AUC values indicate high reliability of the prediction (Supplementary Figure 2B–2D).

High expression of ADAR was significantly associated with poor DSS in ACC (HR = 2.80207, $P = 0.0141$), KIRP (HR = 2.60391, $P = 0.0222$), and LGG (HR = 1.76521, $P = 0.0052$) (Supplementary Figure 3A). This conclusion was further tested by risk distribution analysis, survival analysis, and ROC curve analysis (Supplementary Figure 3B–3D). In addition, Cox regression analysis was performed to investigate the impact of ADAR on pan-cancer PFS and DFS, and the results proved that ADAR was associated with worse PFS in ACC (HR = 2.96237, $P = 0.0011$), KICH (HR = 5.18454, $P = 0.0355$), KIRO (HR = 1.77391, $P = 0.0364$), LGG (HR = 1.33619, $P = 0.0486$) and UCEC (HR = 1.46373, $P = 0.0357$) and predicted better PFS in KIRC (HR = 0.70511, $P = 0.0301$). Similarly, high ADAR expression predicted poor DFS in CESC (HR = 2.41896, $P = 0.0378$) and KIRP (HR = 4.84632, $P = 0.0015$) but was positively associated with better DFS in LGG (HR = 0.3786, $P = 0.0386$) (Supplementary Figure 4A, 4B).

Mutational landscape of ADAR in pan-cancer

We observed the genetic alteration status of ADAR across cancers through the cBioPortal database. ADAR gained the highest alteration frequency in breast cancer and was dominated by amplification. In endometrial

cancer, bladder cancer and uterine endometrioid carcinoma, almost all ADAR gene alterations were amplification (Figure 2A). The types, loci, and case information of ADAR genetic alterations are shown in Figure 2B. We found missense mutations represented by the S629F mutation to be the predominant type of genetic alteration in ADAR. The 3D structure also shows the S629F mutation site on the ADAR protein

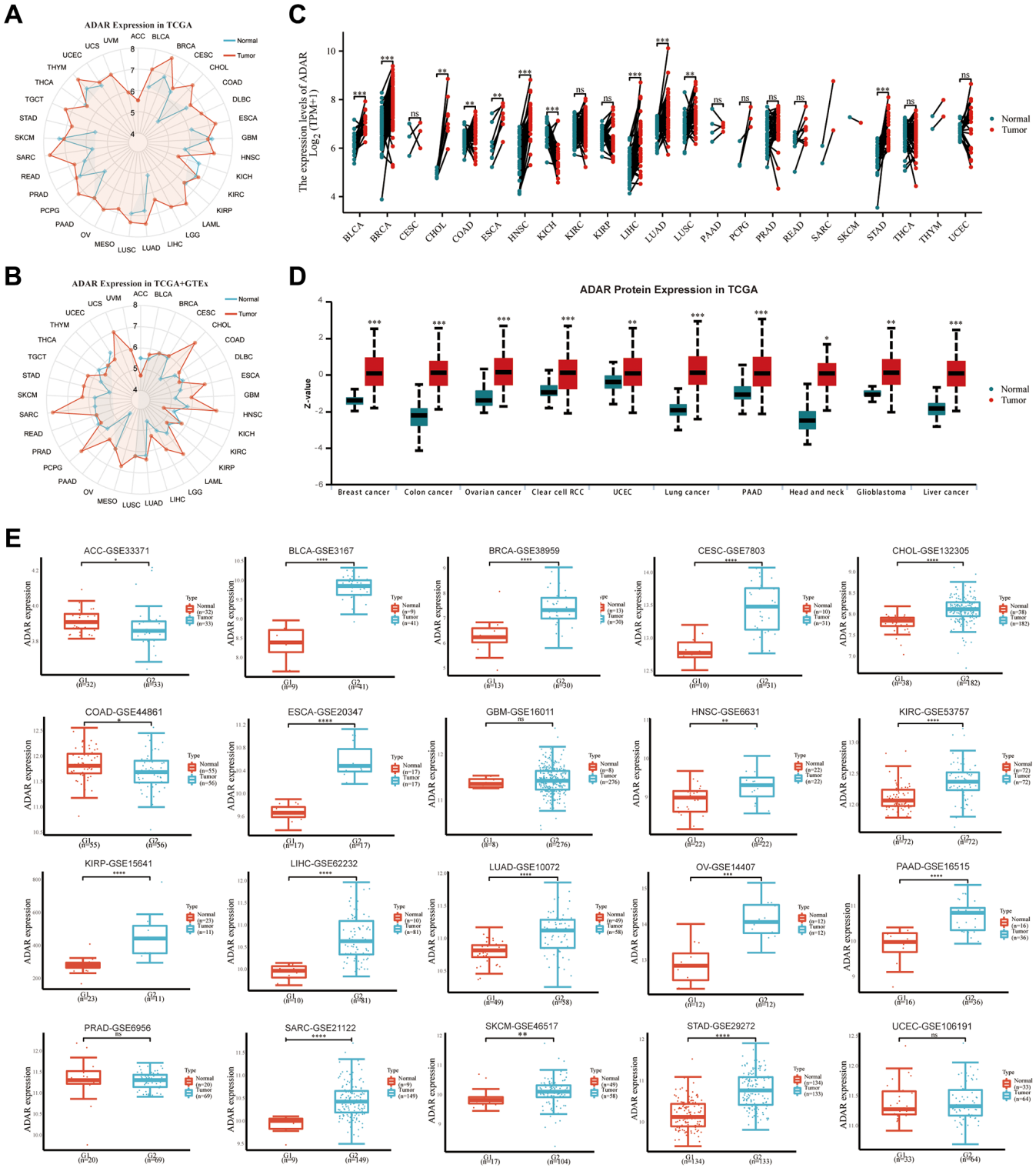

Figure 1. ADAR is upregulated in most cancers. (**A**) ADAR expression of pan-cancer in TCGA database. (**B**) ADAR expression of pan-cancer in TCGA database combined with GTEx database. (**C**) Pairing difference analysis of ADAR in TCGA database. (**D**) ADAR protein levels are significantly elevated in a variety of cancers. (**E**) ADAR expression of pan-cancer in GEO database.

(Figure 2C). Subsequently, we generated a dot plot of ADAR gene alterations across cancers. Most cancers were dominated by amplification (Figure 2D). However, there was no significant difference in survival analysis between the altered and unaltered groups (Figure 2E).

Interaction network of ADAR and enrichment analysis of related genes

Fifty experimentally verified ADAR-interacting genes were obtained from the String database and are presented in Figure 3A. We subsequently obtained a list

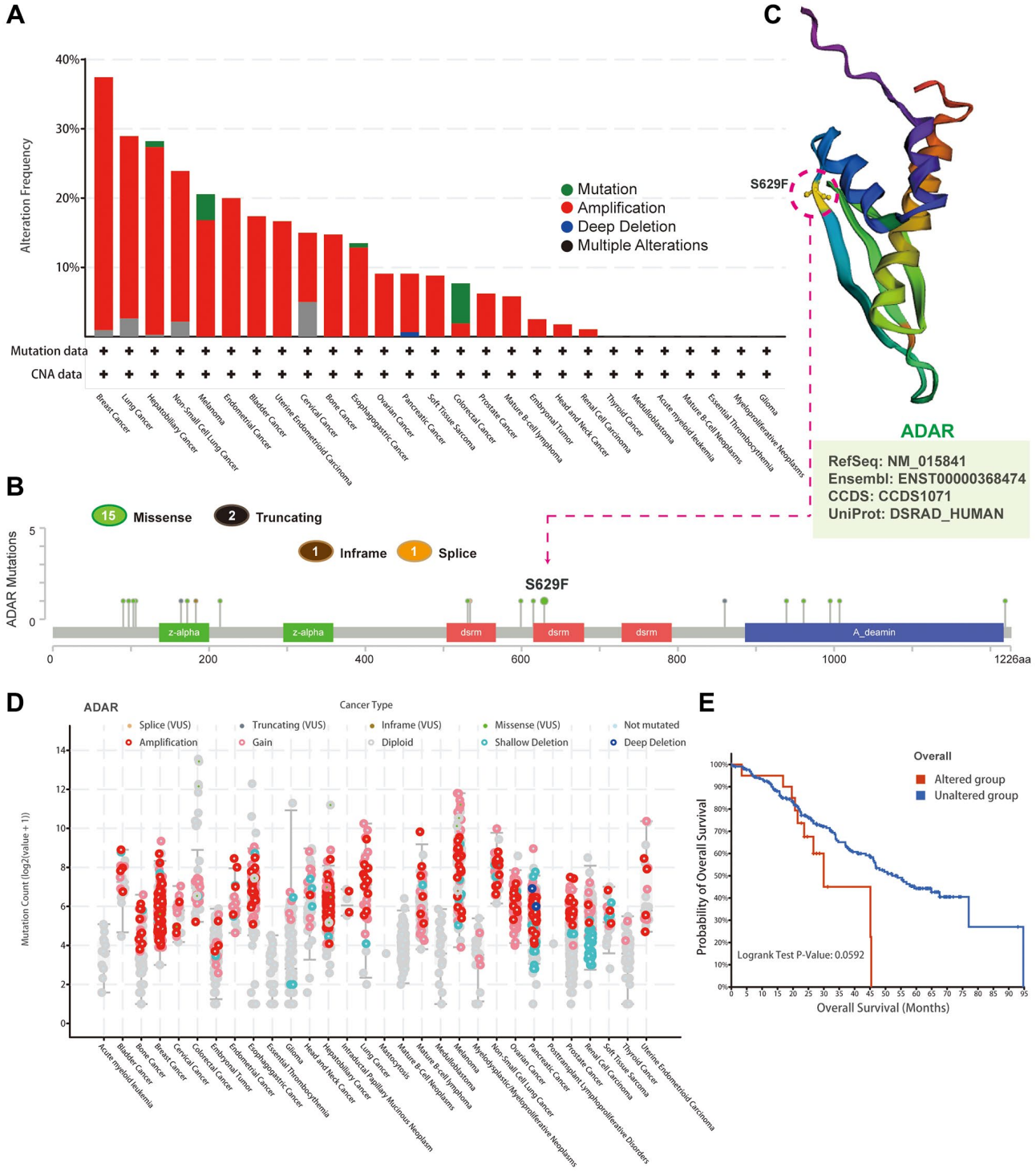

Figure 2. Mutational landscape of ADAR in pan-cancer. (**A**) The genetic alteration status of ADAR in pan-cancer through the cBioPortal database. (**B**) The types, loci, and case information of ADAR genetic alterations. (**C**) The 3D structure shows the S629F mutation site on ADAR protein. (**D**) A dot plot of ADAR gene alterations in pan-cancer. (**E**) Survival analysis between the altered and unaltered groups.

of the top 100 ADAR-related genes from the GEPIA 2.0 website (Supplementary Table 1). Figure 3B presents a heatmap of the specific associations of the five most highly correlated ADAR genes (EIF2AK2, ISG20L2, SMG7, UBAP2L, and YY1AP1) in pan-cancer. To obtain the genes most associated with ADAR, we performed intersection analysis of these two gene sets. The Venn map showed that EIF2AK2 was the most critical gene. We also presented correlations for EIF2AK2 and four additional significantly associated genes (Figure 3C). Subsequently, we performed GO and KEGG enrichment analyses for all ADAR-related genes. Among them, response to virus and RNA binding were the main enrichment functions (Figure 3D). GSEA revealed the molecular pathways of ADAR-related genes enriched in BLCA, BRCA, CESC, and UCEC, with the response of EIF2AK4 Gcn2 to amino acid deficiency, eukaryotic translation elongation, ribosomes, and cytoplasmic ribosomal proteins significantly enriched in both BLCA and CESC (Figure 3E).

Significant correlation between ADAR expression and immune infiltration of cancers

Analysis of the correlation between ADAR expression and immune infiltration of cancer revealed that ADAR was correlated with the number of immune cells in most tumors, with the most significant positive correlation with the infiltration of M1 macrophages (Figure 4A). Furthermore, in the HPA single-cell dataset, correlation analysis between ADAR expression and immune cell clustering revealed that ADAR is a part of cluster-1 (T cells—immune response), with high annotation reliability (Figure 4B, 4C, Supplementary Table 2). Gene ontology treemap describes that ADAR is significantly correlated with immune response and T cell activation, differentiation, and proliferation (Figure 4D). It is worth noting that ADAR and Treg cells showed obvious negative correlations in a variety of cancers, such as BLCA, BRCA, COAD, KIRP, READ, SKCM, STAD, THYM, and UCEC. A positive correlation was only shown in

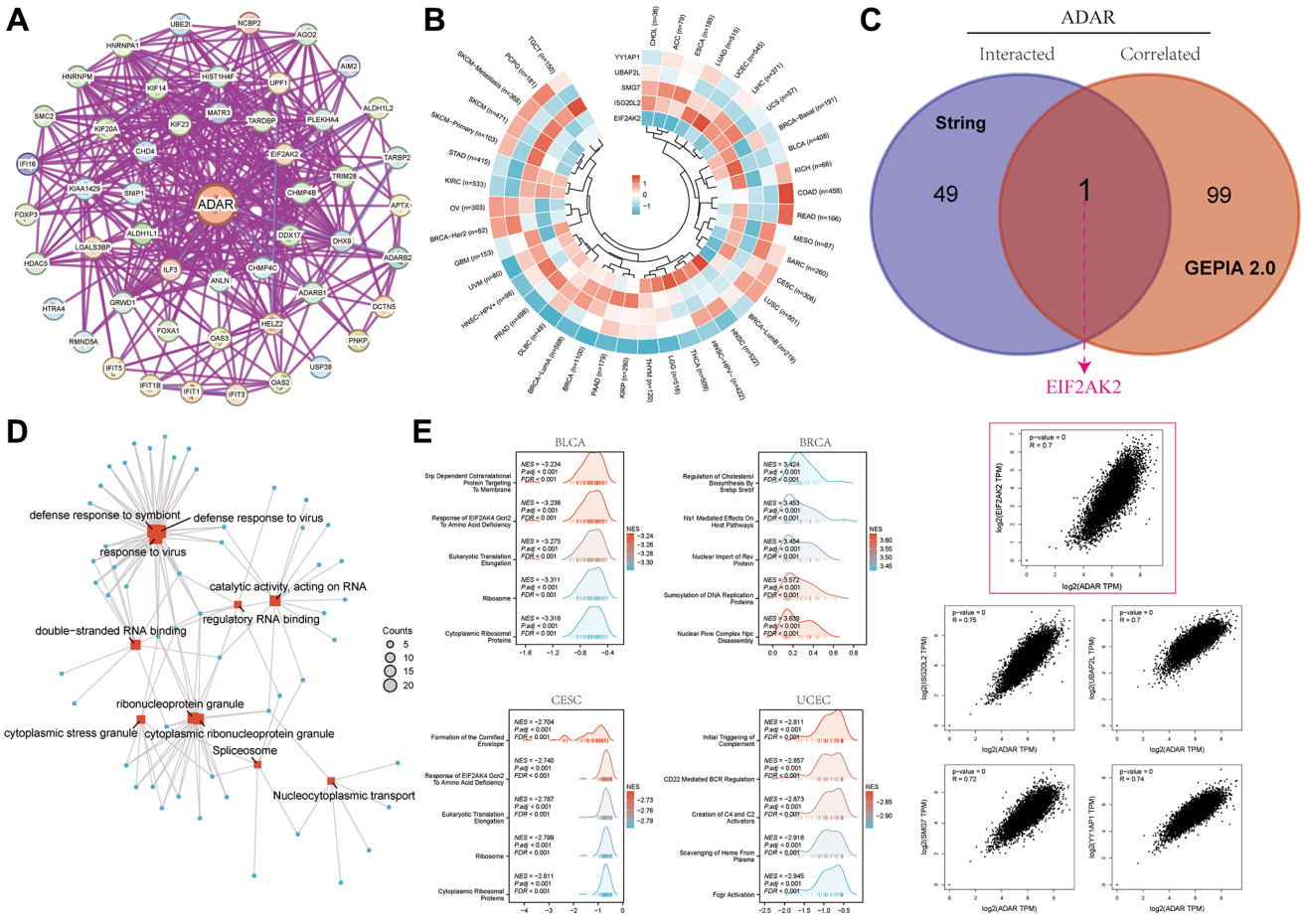

Figure 3. Interaction network of ADAR and enrichment analysis of related genes. (**A**) 50 experimentally verified ADAR interacting genes obtained from the String database. (**B**) A heat map of the specific associations of the five most highly correlated ADAR genes (EIF2AK2, ISG20L2, SMG7, UBAP2L, and YY1AP1) in pan-cancer. (**C**) EIF2AK2 was the most critical gene. We also presented correlations for EIF2AK2 and four additional significantly associated genes. (**D**) GO and KEGG enrichment analyses for all ADAR-related genes. (**E**) GSEA enrichment analysis revealed the molecular pathways of ADAR-related genes.

LUSC. In BLCA, LUSC, and UVM, ADAR and CD8+ T cells showed a strong positive correlation. However, strong inverse associations were observed in ACC, BRCA, LGG, PRAD, TICH, THYM, and UCEC. Meanwhile, ADAR was found to be positively correlated with the immune score and stromal score of some cancers, such as BLCA, COAD, HNSC, KIRC, OSCC, and PDAC. Negative correlations were observed

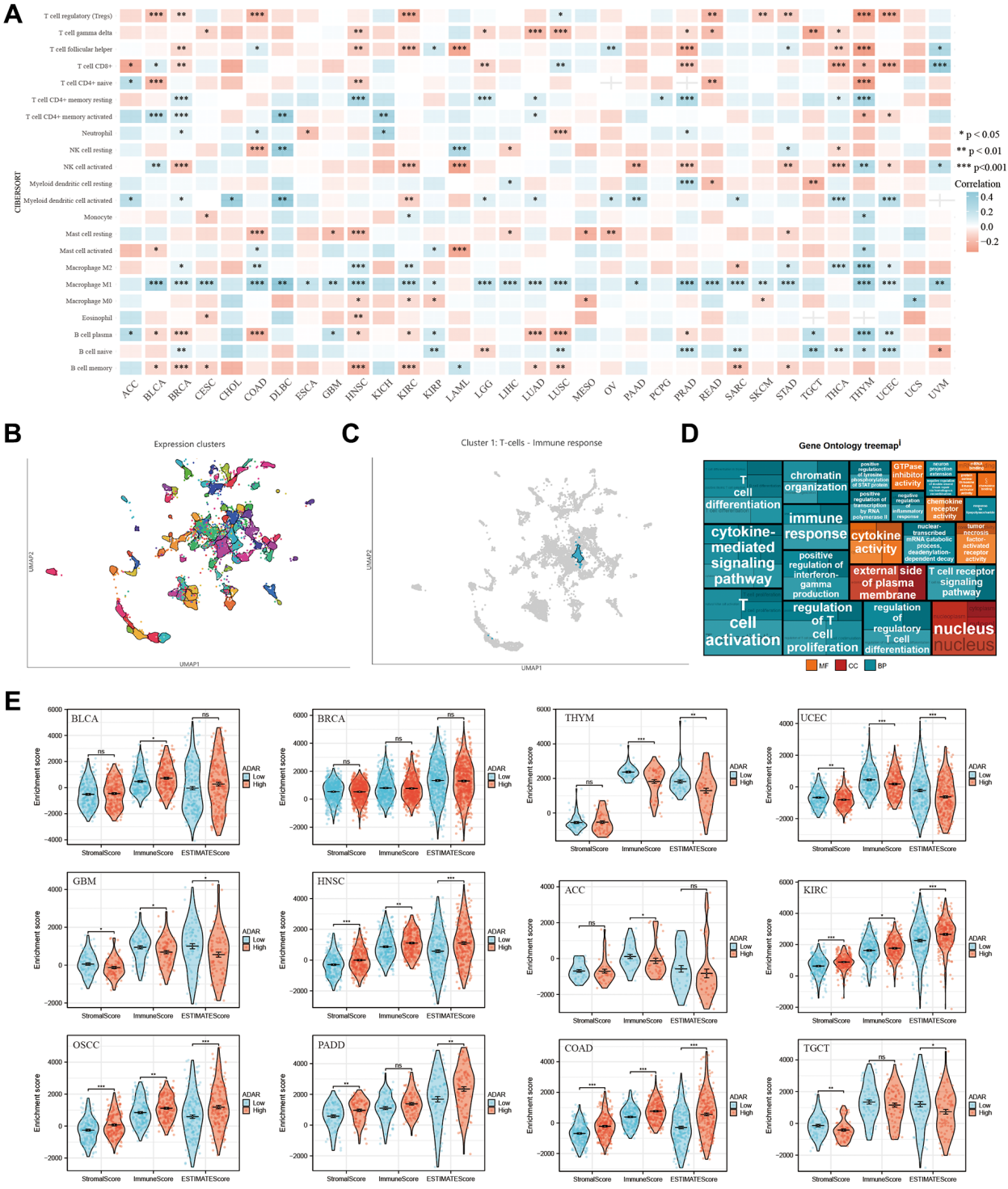

Figure 4. Correlation between ADAR Expression and immune infiltration of cancers. (**A**) ADAR was correlated with the number of immune cells in most tumors. (**B**, **C**) In the HPA single-cell dataset, correlation analysis between ADAR expression and immune cell clustering revealed that ADAR is a part of cluster-1 (T cells—immune response), with high annotation reliability. (**D**) Gene ontology treemap describes that ADAR is significantly correlated with immune response and T cell activation, differentiation, and proliferation. (**E**) Negative correlations were observed in ACC, GBM, TGCT, THYM, and UCEC.

in ACC, GBM, TGCT, THYM, and UCEC (Figure 4E). This indicates the complexity of the regulatory mechanisms of the tumor immune microenvironment and the functional diversity of ADAR.

Involvement of ADAR in the tumor immune response

In cancer, chemokines play a key role in the pattern of immune cell migration into tumors [17]. Human leukocyte antigen (HLA), also known as major histocompatibility complex (MHC), is a protein molecule that exists on the surface of antigen-presenting cells and is responsible for antigen presentation [18]. HLA has been reported to predict the response and prognosis of immunotherapy [19]. Our results show that ADAR is positively correlated with the expression of chemokines, chemokine receptors, HLAs, and tumor necrosis factors (TNFs) in most cancers (Figure 5A–5D). Among them, the most significant genes were CCR1, CCR4, CCR8, XCR1, CXCL10, CXCL11, HLA-E, ENTPD1, IL6R, etc.

ICIs (especially PD-1), TMB, and MSI are now being used as predictive markers of response to immunotherapy [20–22]. Correlation analysis between ADAR and ICI expression showed a highly positive correlation in most cancers (Figure 5E). These findings, especially for BLCA, COAD, and UVM, suggest that ADAR is involved in the regulation of tumor immune responses through the regulation of ICIs. ADAR and TMB achieved a high positive correlation in THYM, ACC, LUAD, STAD, LGG, COAD, KICH, CHOL, SARC, and BLCA (Figure 5F). ADAR was significantly associated with MSI in READ, LAML, COAD, GBM, UVM, CESC, UCEC, LUSC, BLCA, and LIHC (Figure 5G).

Potential functions and molecular pathways of ADAR in BLCA

From the results of the above analysis, we can see that BLCA has the most significant upregulation of ADAR with the highest AUC value. Although ADAR appears to have no effect on BLCA survival, the effect of ADAR on the degree of BLCA malignancy had the highest confidence. Therefore, it is necessary to further explore the potential role of ADAR in BLCA, especially its potential value in BLCA immunotherapy.

Table 1 presents a multivariable Cox regression of ADAR and clinical features of BLCA in TCGA. We can conclude that ADAR is associated with a higher immunotherapy response and predicts a more malignant grade of BLCA ($P = 0.014$). We performed differential analysis between the ADAR high-expression group and the ADAR low-expression group. Fifty differentially expressed genes with low expression and 228 differentially expressed genes with high expression were obtained (Supplementary Table 3). The KRT and CXCL gene families showed significant positive correlations with ADAR (Figure 6A). The gene mutation landscape of the ADAR high- and low-expression groups indicated that the high ADAR expression group predicted a higher frequency of gene mutations (Figure 6B). GO and KEGG enrichment analyses of differentially expressed genes showed that the highly expressed ADAR group was significantly enriched in Epstein Barr virus infection and influenza A pathways; it was also related to the defense response to virus and response to virus (Figure 6C). The ADAR low expression group showed enrichment of the PPAR signaling pathway, aldosterone-regulated sodium reabsorption, sodium ion transmembrane transport, fatty acid derivative metabolic process and other pathways and functions (Figure 6D).

Great value of ADAR in the immunotherapy of BLCA

Tumor immunotherapy has become the focus of discussion among oncologists. Therefore, it is important to explore the potential immunotherapy response markers of BLCA. We explored the immune cell infiltration landscape of cancer samples with the highest ADAR expression (TCGA-FD-A3SR-01, TCGA−FD−A3SR−01, TCGA−GC−A3RB−01) and the lowest ADAR expression (TCGA-CF-A3MI-01, TCGA−CF−A47T−01, and TCGA−ZF−A9R4−01) in TCGA-BLCA using the Timer 2.0 database. In general, the ADAR high expression group had a higher number of immune cells in the tumor microenvironment (Figure 7A). Among them, CD4+ T cells accounted for a greater proportion of patients with high expression of ADAR (Figure 7B). Subsequently, separate analyses targeting the responsiveness of samples with the highest and lowest ADAR expression to immunotherapy revealed that ADAR contributed to higher immunotherapy responses (Figure 7C, 7D). This is consistent with the above conclusion that ADAR is positively correlated with PD-1, CTLA4, and PD-L1. Subsequently, IPSs on all TCGA-BLCA samples reconfirmed that ADAR does not significantly reflect the efficacy of CTLA4-independent immunotherapy. However, when PD1 immunotherapy was used alone or in combination, the high ADAR expression group showed a higher therapeutic benefit. This suggests that ADAR can be used as a superior response marker for PD1 immunotherapy (the recommended immunotherapy strategy for patients with muscle-invasive and metastatic BLCA [23] in patients with BLCA (Figure 7E). The difference boxplot from the immunotherapy cohort IMvigor210 ($n = 348$) showed

that the expression of ADAR in the complete response (CR) group was significantly higher than that in the progressive disease (PD) and stable disease (SD) groups but not significantly different from that in the partial response (PR) group (Figure 7F). Survival analysis showed that patients in the PR and CR groups had significantly better survival expectations than those in the PD and SD groups (Figure 7G). The same results were obtained in another immunotherapy cohort, GSE176307 (n = 90) (Figure 7H, 7I).

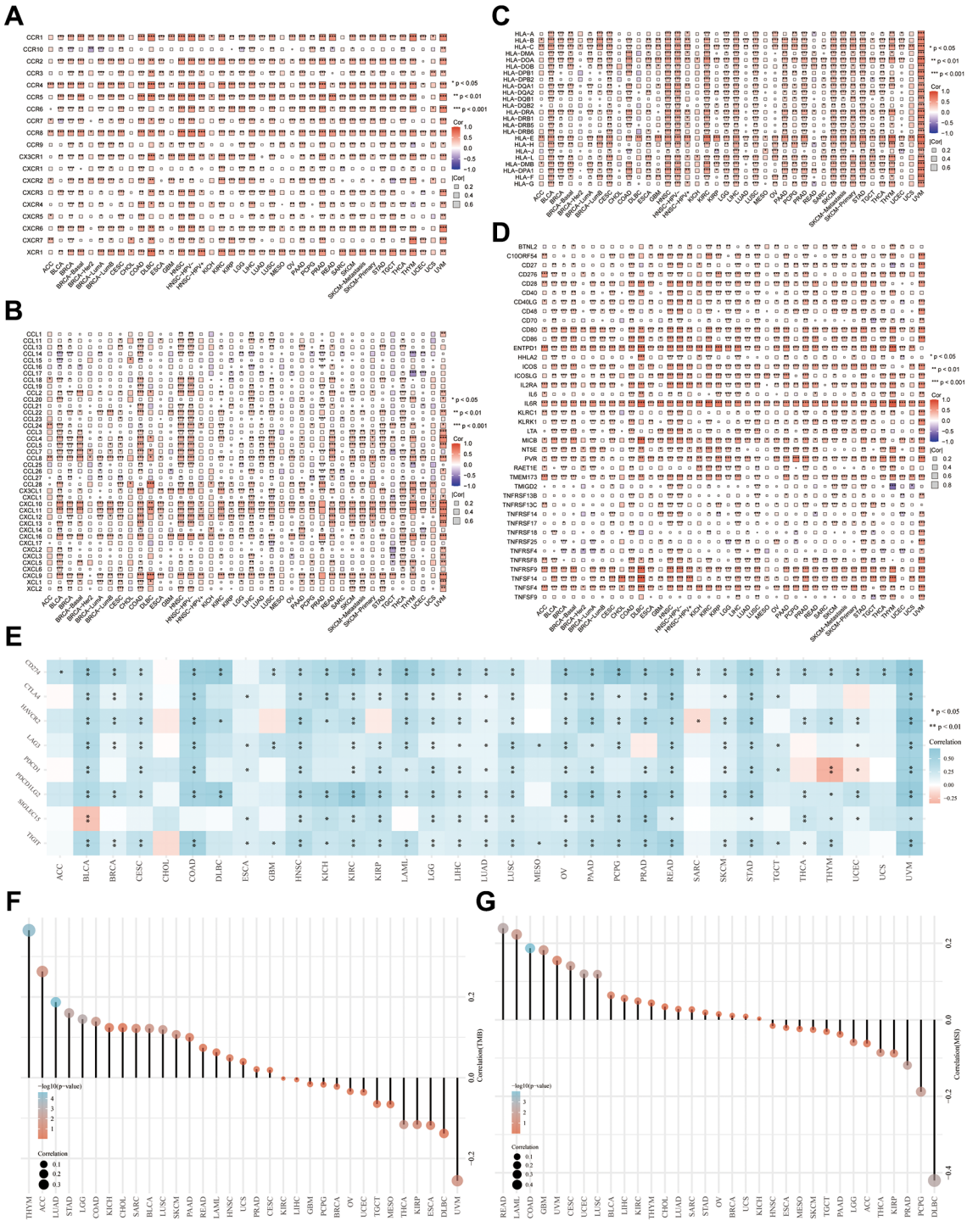

Figure 5. Involvement of ADAR in tumor immune response. (**A**–**D**) ADAR is positively correlated with the expression of chemokines, chemokine receptors, HLAs, and tumor necrosis factors (TNF) in most cancers. (**E**) Correlation analysis between ADAR and ICIs. (**F**) ADAR and TMB achieved high positive correlation in THYM, ACC, LUAD, STAD, LGG, COAD, KICH, CHOL, SARC, and BLCA. (**G**) ADAR was significantly associated with MSI in READ, LAML, COAD, GBM, UVM, CESC, UCEC, LUSC, BLCA, and LIHC.

Table 1. Multivariable Cox regression of ADAR and clinical features of BLCA in TCGA.

Characteristics	Low expression of ADAR	High expression of ADAR	*P*-value
n	206	206	
Age, *n* (%)			0.112
≤70	108 (26.2%)	124 (30.1%)	
>70	98 (23.8%)	82 (19.9%)	
Gender, *n* (%)			0.502
Female	51 (12.4%)	57 (13.8%)	
Male	155 (37.6%)	149 (36.2%)	
Primary therapy outcome, *n* (%)			0.032
PD	29 (8.2%)	41 (11.5%)	
SD	10 (2.8%)	20 (5.6%)	
PR	15 (4.2%)	7 (2%)	
CR	122 (34.4%)	111 (31.3%)	
Histologic grade, *n* (%)			0.014
Low grade	16 (3.9%)	5 (1.2%)	
High grade	189 (46.2%)	199 (48.7%)	
Pathologic stage, *n* (%)			0.560
Stage I	1 (0.2%)	3 (0.7%)	
Stage II	65 (15.9%)	64 (15.6%)	
Stage III	67 (16.3%)	75 (18.3%)	
Stage IV	72 (17.6%)	63 (15.4%)	
Smoker, *n* (%)			0.052
No	63 (15.8%)	46 (11.5%)	
Yes	136 (34.1%)	154 (38.6%)	
OS event, *n* (%)			0.321
Alive	120 (29.1%)	110 (26.7%)	
Dead	86 (20.9%)	96 (23.3%)	

Validation of ADAR expression and function in BLCA

By bioinformatics analysis, we identified the important role of ADAR in BLCA, especially as a biomarker for the progression and response to immunotherapy. For more reliable verification, we further confirmed the expression and function of ADAR in BLCA by experiments. We examined the expression of ADAR in bladder cancer tissues ($n = 40$) and matched adjacent normal tissues ($n = 40$) by qRT-PCR. ADAR was significantly upregulated in bladder cancer tissues, which was consistent with the bioinformatics analysis results (Figure 8A). The protein levels of ADAR in 8 pairs of bladder cancer tissues (T) and adjacent normal tissues (N) were detected by western blotting, and the results were consistent with those obtained by qRT-PCR (Figure 8B). ADAR was also upregulated in five bladder cancer cell lines (T24, RT4, 5637, 253J and BIU87) compared with SVHUC-1 (human ureteral epithelial immortalized cell line, as the normal urothelial cell line) (Figure 8C). We subsequently performed IHC analysis of bladder cancer tissues from 180 patients, and Figure 8D shows pictures of the results with high and low ADAR expression. The survival analysis revealed that ADAR is a risk factor for BLCA and predicts poor survival expectations (Figure 8E). These data suggest that ADAR is upregulated in BLCA and is detrimental for survival. Table 2 presents correlations between the expression of ADAR and clinicopathological features in the 180 BLCA patients. We can conclude that the high expression of ADAR is positively correlated with the histological grade (<0.001) and Tumor size ($P = 0.017$) of bladder cancer. In addition, the higher the ADAR expression, the larger the predicted tumor ($P = 0.0079$). To further investigate the functional effects of ADAR on bladder cancer cells, we selected high-grade bladder cancer cell line T24 and low-grade bladder cancer cell line BIU87 to conduct experimental verification. ADAR was knocked down/overexpressed in T24 cells and BIU87 cells. Figure 8F–8I shows knockdown/overexpression efficiency of ADAR.

CCK-8 assays showed that ADAR knockdown significantly inhibited the proliferation of bladder cancer cells (Figure 9A). However, overexpression of ADAR had the opposite effect (Figure 9B). Colony assays showed that inhibition of ADAR significantly reduced the clone numbers of T24 cells and BIU87 cells (Figure 9C). However, the opposite results were observed when ADAR was upregulated (Figure 9D). These results suggest that ADAR can promote the proliferation of bladder cancer cells. In addition, invasion assays (Transwell) were performed in T24 and BIU87 cell lines. Knockdown of ADAR inhibited the

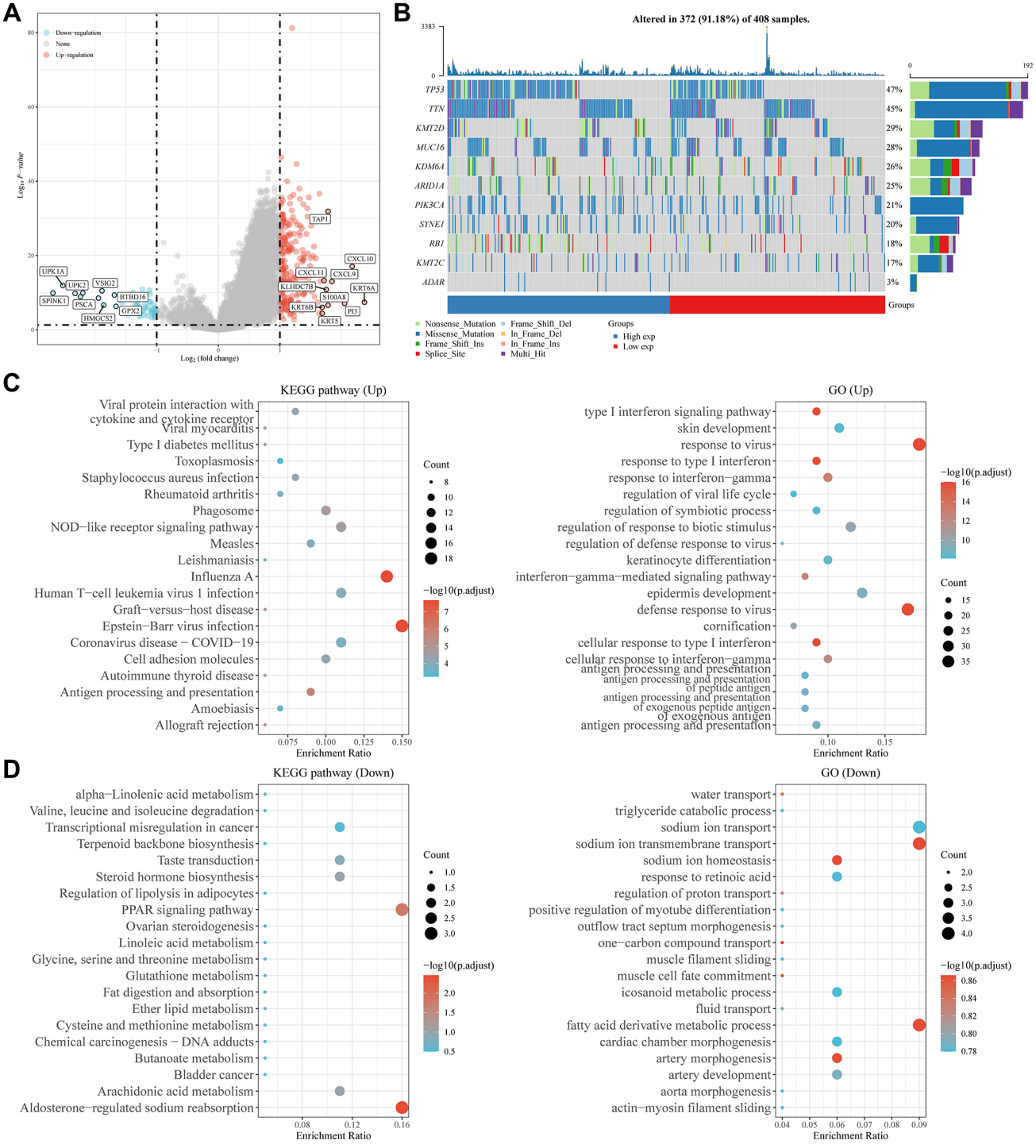

Figure 6. Potential functions and molecular pathways of ADAR in BLCA. (**A**) Differential analysis between the ADAR high-expression group and the ADAR low-expression group. (**B**) High ADAR expression predicts a higher frequency of gene mutations. (**C**, **D**) GO and KEGG enrichment analysis of differentially expressed genes.

invasion of T24 and BIU87 cells (Figure 9E). Overexpression of ADAR promoted the invasion of T24 and BIU87 cells (Figure 9F). Finally, we performed a migration assay (wound healing), and the results showed that downregulation of ADAR inhibited the migration ability of bladder cancer cells, while upregulation of ADAR achieved the opposite effect (Figure 9G, 9H). Taken together, these *in vitro*

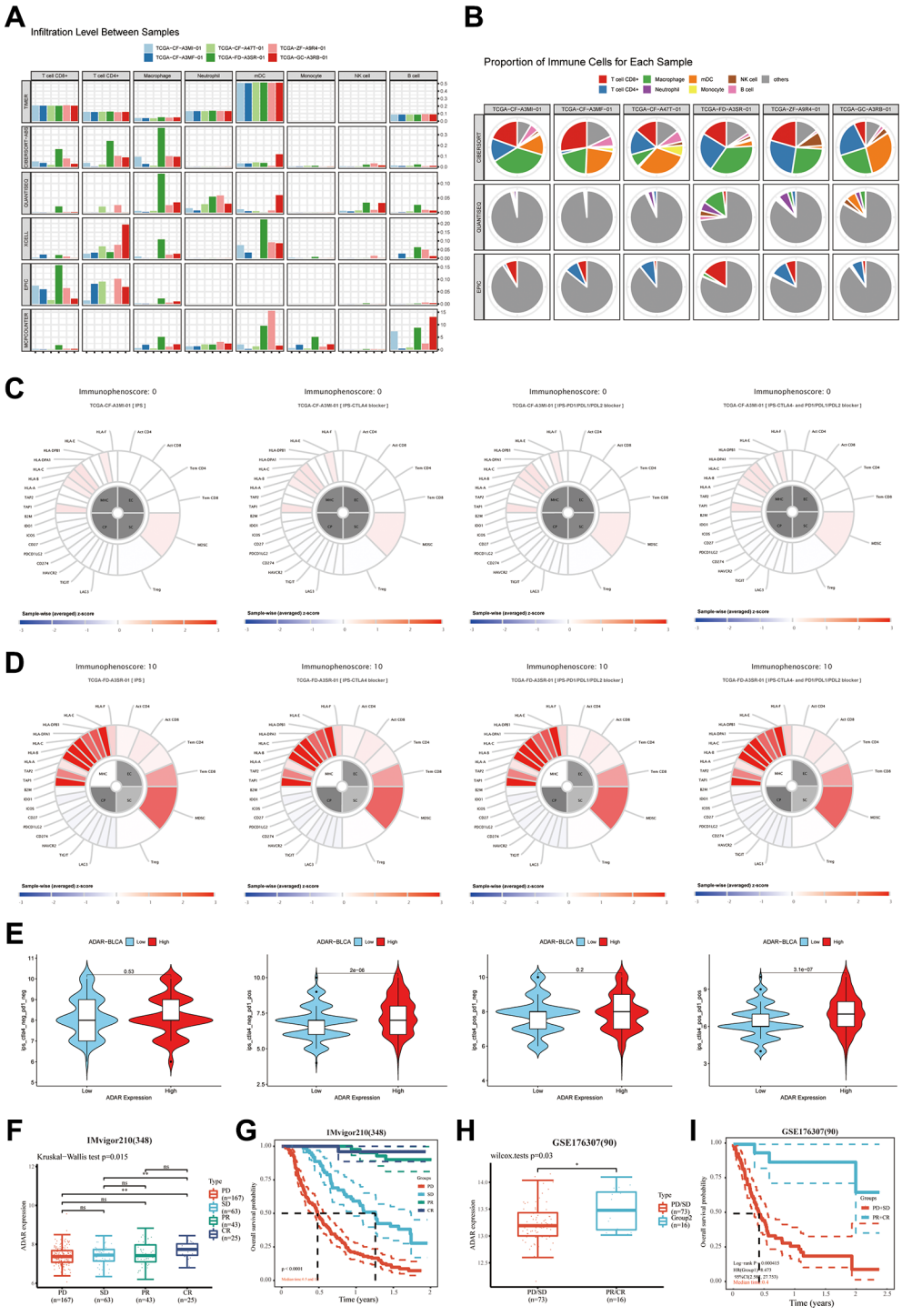

Figure 7. The great value of ADAR in the immunotherapy of BLCA. (**A**) The ADAR high expression group had a higher number of immune cells in the tumor microenvironment. (**B**) CD4+T cells accounted for a greater proportion of patients with high expression of ADAR. (**C**, **D**) ADAR contribute to higher immunotherapy responses. (**E**) IPS scores on all TCGA-BLCA samples reconfirmed the conclusion that high ADAR expression predicted a better immunotherapy response. (**F**) The difference boxplot from the immunotherapy cohort IMvigor210 (*n* = 348). (**G**) Survival analysis showed that patients in PR and CR groups had significantly better survival expectations than those in PD and SD groups. (**H**, **I**) The difference boxplot and survival analysis from the immunotherapy cohort GSE176307 (*n* = 90).

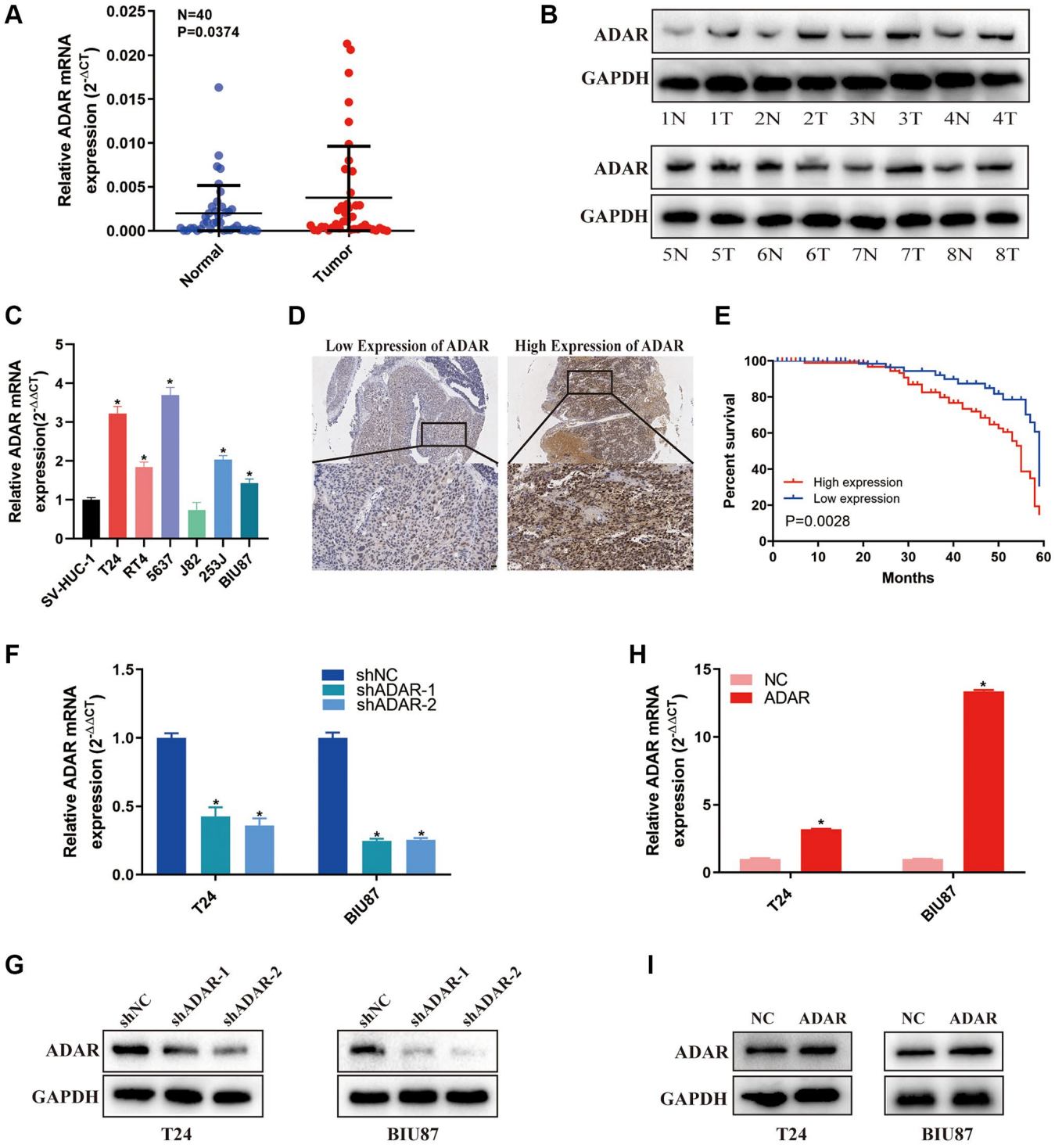

Figure 8. ADAR was up-regulated in bladder cancer tissues and served as a prognostic factor in bladder cancer. (**A**) Relative expression of ADAR mRNA in the 40 pairs of bladder cancer tissues and matched adjacent normal tissues quantified by qRT-PCR. ADAR was up-regulated in bladder cancer tissues compared with that in adjacent normal tissues. (**B**) The expression of ADAR protein in 8 pair bladder cancer tissues (T) and adjacent normal tissues (N) by western blot were shown. (**C**) Relative expression of ADAR in bladder cancer cell lines and normal bladder epithelial cell line SV-HUC-1 by qRT-PCR. Data represent the mean ± SD from three independent experiments, $^{*}P < 0.05$. (**D**) IHC analysis of ADAR in bladder cancer tissue at 100× and 400× magnification. (**E**) Kaplan-Meier survival curves of overall survival in 180 bladder cancer patients based on ADAR by IHC staining. The log-rank test was used to compare differences between two groups ($P = 0.0028$). (**F**, **G**) Validation of the knockdown efficacy of ADAR in T24 and BIU87 cell lines by qRT-PCR and western blot. Data represent the mean ± SD from three independent experiments, $^{*}P < 0.05$. (**H**, **I**) The overexpression efficacy of ADAR in T24 and BIU87 cell lines by qRT-PCR and western blot. Data represent the mean ± SD from three independent experiments, $^{*}P < 0.05$.

Table 2. Correlations between the expression of ADAR and clinicopathological features in BLCA patients.

Characteristics	Case	ADAR		*P*-value
		Low	High	
All cases, *n* (%)	180	75 (41.7)	105 (58.3)	
Age (years), *n* (%)				0.803
<65	39	16 (41.0)	23 (59.0)	
≥65	141	61 (43.3)	80 (56.7)	
Gender, *n* (%)				0.772
Male	133	59 (44.4)	74 (55.6)	
Female	47	22 (46.8)	25 (53.2)	
TNM stage, *n* (%)				0.938
pTa-pT1	104	35 (33.7)	69 (66.3)	
pT2-pT4	76	26 (34.2)	50 (65.8)	
Histological grade				<0.001*
Low	117	72 (61.5)	45 (38.5)	
High	63	17 (27.0)	46 (73.0)	
Tumor size (cm)				0.017*
<3	103	56 (54.4)	47 (45.6)	
≥3	77	28 (36.4)	49 (63.6)	

*$P < 0.05$.

experiments demonstrated that ADAR plays a key role in promoting the proliferation, migration, and invasion of bladder cancer cells, thus promoting the progression of BLCA.

DISCUSSION

Cancer seriously affects human health and is now the second leading cause of death worldwide. Tumor therapy mainly includes traditional surgical therapy, radiotherapy, chemotherapy and new therapies such as targeted therapy and immunotherapy, which have developed rapidly in recent years. In addition, the combination of next-generation sequencing and advanced computational data analysis methods has revolutionized our understanding of the genomic basis of cancer development and progression [24]. Pan-cancer bioinformatics analysis of these data allows us to understand the major pathological functions and mechanisms of a key gene and explore its role and potential clinical value in tumorigenesis, progression, and treatment response in a specific cancer. ADAR has been shown to be a central protein involved in RNA editing [25]. However, the potential oncogenic effects of ADAR and its value in tumor therapy deserve further investigation and exploration. In this study, we systematically elucidated the integrated landscape of ADAR in cancer. By combining different bioinformatics platforms and datasets from different sources, we comprehensively analyzed the differential expression, prognostic significance, mutation landscape, gene interaction network, regulation of ADAR in the tumor microenvironment, and predictive value in cancer immunotherapy. We hope that this study will provide new insights into improving the role of ADAR in cancer and tumor immunotherapy.

Previous studies have reported that dysregulation of ADAR is closely related to carcinogenesis and malignant progression of tumors. For example, ADAR can promote the development of thyroid cancer through RNA editing of CDK13 [26]. Inhibition of ADAR expression can significantly inhibit the proliferation, invasion and migration of thyroid cancer cells, reflecting the strong carcinogenic effect of ADAR [27]. Based on these clues, we comprehensively explored the expression of ADAR across cancers. We found that ADAR mRNA and protein expression was significantly higher in most tumor tissues than in normal tissues. In addition, high expression of ADAR predicts a higher pathological grade. Furthermore, ADAR is associated with the survival of patients with a variety of cancers. For example, high expression of ADAR predicts poor overall survival in ACC, KICH, and LGG. Similarly, PFS, DSS, and DFS analyses showed that ADAR was an unfavorable factor for tumor patients. Therefore, it is

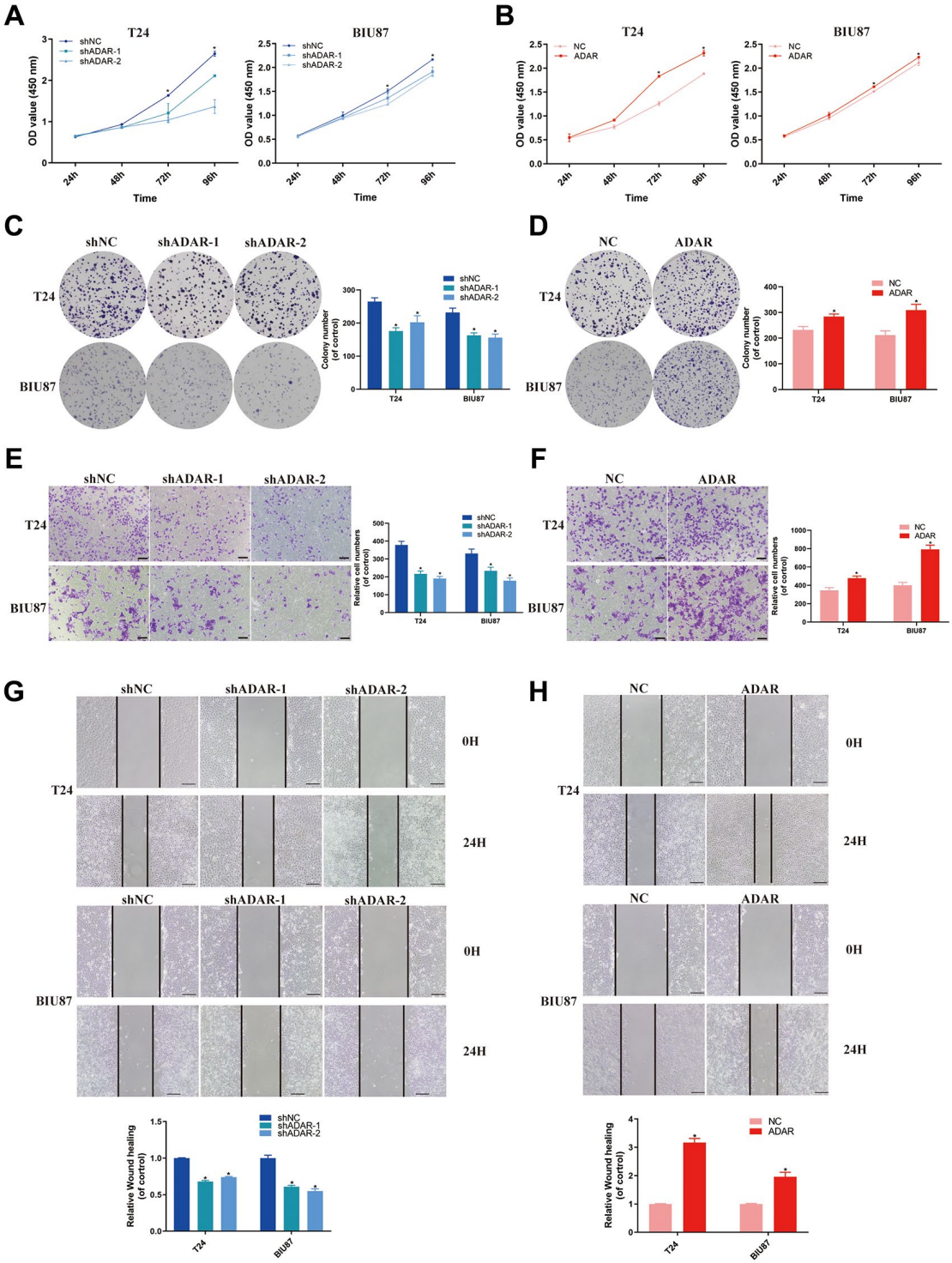

Figure 9. ADAR promoted bladder cancer cell proliferation, invasion and migration *in vitro*. (**A**, **B**) Cell proliferation assessed by CCK8 assays. Knockdown of ADAR inhibited cell proliferation in T24 and BIU87 cells. Overexpression of ADAR promoted cell proliferation in T24 and BIU87 cells. Data represent the mean ± SD from three independent experiments, $^{*}P < 0.05$. (**C**, **D**) Colony formation assay showed that knockdown of ADAR significantly decreased the cloning number of T24 and BIU87 cells compared with control group, while ADAR overexpression significantly increased the cloning number of T24 and BIU87 cells. Data represent the mean ± SD from three independent experiments, $^{*}P < 0.05$. (**E**, **F**) Invasion assay (Transwell) in T24 and BIU87 cell lines were measured. The results were expressed of crossing cells number per field compared with respective control. Magnification: 100×. Data represent the mean ± SD from three independent experiments, $^{*}P < 0.05$. (**G**, **H**) Migration assay (Wound healing) in T24 and BIU87 cell lines were measured. Knockdown of ADAR inhibited cell migration in T24 and BIU87 cells after 24 hours. Overexpression of ADAR promoted cell migration in T24 and BIU87 cells after 24 hours. Data represent the mean ± SD from three independent experiments, $^{*}P < 0.05$.

of great value to explore ADAR for tumor prediction and diagnosis. 8-Azaadenosine is a potent ADAR1 inhibitor and an A-to-I editing inhibitor. It has been verified by experiments that 8-azaadenosine can inhibit the proliferation of thyroid cancer cells and suppress the progression and peritoneal metastasis of gastric cancer by inhibiting ADAR [27, 28]. The clinical value of 8-azaadenosine will be realized by its combination with existing cancer treatment drugs.

The activation or alteration of signaling pathways is fundamental to disease occurrence [29]. Oncogenes or tumor suppressor genes lead to the initiation or attenuation of cancer by affecting their downstream signaling pathways. Enrichment analysis showed that ADAR and its interacting genes were mainly involved in immune and tumor-related pathways such as response to viruses, spliceosome formation and regulatory RNA binding. This is consistent with previous research reports that ADAR-induced deamination of RNA is a significant source of mutant SARS-CoV-2 [30]. These results suggest that ADAR is closely related to cancer development and immunity.

Furthermore, we evaluated the pan-cancer immune infiltration landscape and found that ADAR was associated with infiltrating immune cells. The tumor immune microenvironment is mainly composed of tumor cells, stromal cells and immune cells. As one of the main components, immune cells play an important role in antitumor immunity and protumor immunity [31]. Oncogenes or tumor suppressor genes can participate in the reconstruction of the tumor immune microenvironment by regulating immune cells, thereby inhibiting or promoting antitumor immunity [32]. One study showed that the deletion of PTPN2 phosphatase in T cells promotes antitumor immunity and CAR T-cell efficacy in solid tumors [33]. Another study demonstrated that ADAR promotes T-cell migration to human melanoma cells [34]. In addition, ADAR has been shown to improve Treg cell function via the miR-21b/Foxp3 axis [35]. Our study showed that ADAR is associated with the activation of M1 macrophages. This evidence indicates the regulatory effect of ADAR on immune cells in the tumor microenvironment. We also revealed the relationship between ADAR and chemokines, chemokine receptors, and other immune-related factors. The complexity of the regulatory network between ADAR and immune microenvironment components suggests that the mechanism of ADAR is multifaceted. The application of immune checkpoint inhibitors (ICIs) has revolutionized the treatment of various cancers. However, despite success in some cancer patients, a significant proportion of patients do not respond to immune checkpoint inhibitors [36]. Our study found that ADAR was positively correlated with the expression of multiple immune checkpoints, which may indicate a favorable response to immunotherapy. TMB and MSI have become effective immunotherapy response markers in cancer. A high TMB means that more tumor neoantigens are exposed, so a high TMB predicts more effective immunotherapy. MSI presents as a DNA mismatch repair defect and is a marker of a good response to immunotherapy [21, 37]. Our study showed that in COAD and BLCA, ADAR was proportional to both TMB and MSI. This shows the clinical value of ADAR as a response marker in the immunotherapy of these two cancers.

ADAR plays an important role in the disease progression and immunotherapy of bladder cancer. However, the specific performance of ADAR in the immunotherapy response of bladder cancer has not yet been reported by urologists, so we chose BLCA to further analyze ADAR. We first investigated the specific molecular pathways by which ADAR may be involved in bladder cancer by bioinformatics analysis. Among them, Epstein Barr virus infection and influenza A pathways were significantly enriched. ADAR has also been found to be associated with the immune response to viruses. In addition, the TCGA-BLCA samples with the highest expression of ADAD showed significantly increased infiltration levels of immune cells such as CD4+ cells, macrophages and DCs. Moreover, the IPS showed that high expression of ADAR predicted a better response to PD-1 blockade in BLCA. This is consistent with the published results of two immunotherapy cohorts (GSE176307 and IMvigor210) of BLCA. We therefore hypothesized that RRM2 may play a role as an immunotherapy predictive marker in BLCA. Furthermore, in our collected clinical samples, ADAR was significantly upregulated in bladder cancer tissues and was associated with poor patient survival. Moreover, *in vitro* experiments showed that ADAR effectively promoted the proliferation, migration, and invasion of bladder cancer cells. Taken together, these results suggest that ADAR is a key regulator and plays an important role in BLCA development, progression, and immunotherapy. With further exploration, ADAR may become a promising therapeutic target for BLCA.

CONCLUSION

In summary, we demonstrated that ADAR is ubiquitously expressed across cancers and is associated with poor clinical outcomes in most cancers. In addition, we illustrated the complex relationship between ADAR and the tumor immune microenvironment and propose the hypothesis that

ADAR may be involved in the regulation of the tumor immunotherapy response. Finally, we propose the important role of ADAR in BLCA, which can be used as a predictive marker for immunotherapy response and as a therapeutic target.

Abbreviations

ADAR: adenosine deaminase acting on RNA; dsRNA: double-stranded RNA; TME: tumor microenvironment; TMB/MSI: tumor mutation burden/microsatellite instability; IPS: immunophenoscore; MHC: MHC molecules; CP: immunomodulators; EC: effector cells; SC: suppressor cells; BLCA: bladder cancer; TCGA: the cancer genome atlas; ICB: immune checkpoint blockade; OS: overall survival; PFS: progression-free survival; DSS: disease-specific survival; RFS: relapse-free survival; HRs: hazard ratios; GO: gene ontology; KEGG: Kyoto encyclopedia of genes and genomes; GSEA: gene set enrichment analysis; GTEx: the genotype-tissue expression; T: tumour size or extension, or both; N: regional lymph node involvement; M: distant metastasis; ROC: receiver operator characteristic curve; AUC: area under the curve; PD-1: programmed cell death protein-1; CTLA-4: cytotoxic T lymphocyte antigen 4; CCL: C-C motif chemokine ligand; CXCL: C-X-C motif chemokine ligand.

AUTHOR CONTRIBUTIONS

XY and QL conceived of the study, carried out its design and performed surgery and provided clinical samples, HWY and QL provodes methodology, experimental equipments and funding for experimental reagents. HY and YDC performed the related bioinformatics analysis. KXB and JCL collected and handled clinical samples and performed the cell experiments. YDC and QS followed up patients' information. HY layouted figures and wrote the first draft of the manuscript. XY and HWY revised the paper. All authors read and approved the final manuscript.

CONFLICTS OF INTEREST

The authors declare that the research was conducted in the absence of any commercial or financial relationships that could be construed as a potential conflict of interest.

ETHICAL STATEMENT AND CONSENT

The patient's informed consent was obtained and the Ethics Committee of the First Affiliated Hospital of Nanjing Medical University approved the protocol used in this study.

FUNDING

This work was supported by the National Natural Science Foundation of China (No. 82273152, 82072832 and 82073306), Jiangsu Province Capability Improvement Project through Science, Technology and Education (No. ZDXK202219) and Postgraduate Research and Practice Innovation Program of Jiangsu Province (No. KYCX21_1607).

REFERENCES

1. Siegel RL, Miller KD, Wagle NS, Jemal A. Cancer statistics, 2023. CA Cancer J Clin. 2023; 73:17–48. https://doi.org/10.3322/caac.21763 PMID:36633525

2. Olagunju A, Forsman T, Ward RC. An update on the use of cryoablation and immunotherapy for breast cancer. Front Immunol. 2022; 13:1026475. https://doi.org/10.3389/fimmu.2022.1026475 PMID:36389815

3. Reck M, Remon J, Hellmann MD. First-Line Immunotherapy for Non-Small-Cell Lung Cancer. J Clin Oncol. 2022; 40:586–97. https://doi.org/10.1200/JCO.21.01497 PMID:34985920

4. Huang AC, Zappasodi R. A decade of checkpoint blockade immunotherapy in melanoma: understanding the molecular basis for immune sensitivity and resistance. Nat Immunol. 2022; 23:660–70. https://doi.org/10.1038/s41590-022-01141-1 PMID:35241833

5. Ganesh K, Stadler ZK, Cercek A, Mendelsohn RB, Shia J, Segal NH, Diaz LA Jr. Immunotherapy in colorectal cancer: rationale, challenges and potential. Nat Rev Gastroenterol Hepatol. 2019; 16:361–75. https://doi.org/10.1038/s41575-019-0126-x PMID:30886395

6. Kennedy LB, Salama AKS. A review of cancer immunotherapy toxicity. CA Cancer J Clin. 2020; 70:86–104. https://doi.org/10.3322/caac.21596 PMID:31944278

7. Zhang Y, Zhang Z. The history and advances in cancer immunotherapy: understanding the characteristics of tumor-infiltrating immune cells and their therapeutic implications. Cell Mol Immunol. 2020; 17:807–21. https://doi.org/10.1038/s41423-020-0488-6 PMID:32612154

8. Vesely MD, Zhang T, Chen L. Resistance Mechanisms to Anti-PD Cancer Immunotherapy. Annu Rev Immunol. 2022; 40:45–74.

https://doi.org/10.1146/annurev-immunol-070621-030155
PMID:35471840

9. Savva YA, Rieder LE, Reenan RA. The ADAR protein family. Genome Biol. 2012; 13:252. https://doi.org/10.1186/gb-2012-13-12-252 PMID:23273215

10. Nishikura K. Editor meets silencer: crosstalk between RNA editing and RNA interference. Nat Rev Mol Cell Biol. 2006; 7:919–31. https://doi.org/10.1038/nrm2061 PMID:17139332

11. Song B, Shiromoto Y, Minakuchi M, Nishikura K. The role of RNA editing enzyme ADAR1 in human disease. Wiley Interdiscip Rev RNA. 2022; 13:e1665. https://doi.org/10.1002/wrna.1665 PMID:34105255

12. Baker AR, Slack FJ. ADAR1 and its implications in cancer development and treatment. Trends Genet. 2022; 38:821–30. https://doi.org/10.1016/j.tig.2022.03.013 PMID:35459560

13. Anadón C, Guil S, Simó-Riudalbas L, Moutinho C, Setien F, Martínez-Cardús A, Moran S, Villanueva A, Calaf M, Vidal A, Lazo PA, Zondervan I, Savola S, et al. Gene amplification-associated overexpression of the RNA editing enzyme ADAR1 enhances human lung tumorigenesis. Oncogene. 2016; 35:4407–13. https://doi.org/10.1038/onc.2015.469 PMID:26640150

14. Kung CP, Cottrell KA, Ryu S, Bramel ER, Kladney RD, Bao EA, Freeman EC, Sabloak T, Maggi L Jr, Weber JD. Evaluating the therapeutic potential of ADAR1 inhibition for triple-negative breast cancer. Oncogene. 2021; 40:189–202. https://doi.org/10.1038/s41388-020-01515-5 PMID:33110236

15. Charoentong P, Finotello F, Angelova M, Mayer C, Efremova M, Rieder D, Hackl H, Trajanoski Z. Pan-cancer Immunogenomic Analyses Reveal Genotype-Immunophenotype Relationships and Predictors of Response to Checkpoint Blockade. Cell Rep. 2017; 18:248–62. https://doi.org/10.1016/j.celrep.2016.12.019 PMID:28052254

16. Jiang P, Gu S, Pan D, Fu J, Sahu A, Hu X, Li Z, Traugh N, Bu X, Li B, Liu J, Freeman GJ, Brown MA, et al. Signatures of T cell dysfunction and exclusion predict cancer immunotherapy response. Nat Med. 2018; 24:1550–8. https://doi.org/10.1038/s41591-018-0136-1 PMID:30127393

17. Ozga AJ, Chow MT, Luster AD. Chemokines and the immune response to cancer. Immunity. 2021; 54:859–74. https://doi.org/10.1016/j.immuni.2021.01.012 PMID:33838745

18. Oelke M, Schneck JP. HLA-Ig-based artificial antigen-presenting cells: setting the terms of engagement. Clin Immunol. 2004; 110:243–51. https://doi.org/10.1016/j.clim.2003.11.014 PMID:15047202

19. Maggs L, Sadagopan A, Moghaddam AS, Ferrone S. HLA class I antigen processing machinery defects in antitumor immunity and immunotherapy. Trends Cancer. 2021; 7:1089–101. https://doi.org/10.1016/j.trecan.2021.07.006 PMID:34489208

20. Bagchi S, Yuan R, Engleman EG. Immune Checkpoint Inhibitors for the Treatment of Cancer: Clinical Impact and Mechanisms of Response and Resistance. Annu Rev Pathol. 2021; 16:223–49. https://doi.org/10.1146/annurev-pathol-042020-042741 PMID:33197221

21. Chan TA, Yarchoan M, Jaffee E, Swanton C, Quezada SA, Stenzinger A, Peters S. Development of tumor mutation burden as an immunotherapy biomarker: utility for the oncology clinic. Ann Oncol. 2019; 30:44–56. https://doi.org/10.1093/annonc/mdy495 PMID:30395155

22. Vilar E, Gruber SB. Microsatellite instability in colorectal cancer-the stable evidence. Nat Rev Clin Oncol. 2010; 7:153–62. https://doi.org/10.1038/nrclinonc.2009.237 PMID:20142816

23. Witjes JA, Bruins HM, Cathomas R, Compérat EM, Cowan NC, Gakis G, Hernández V, Linares Espinós E, Lorch A, Neuzillet Y, Rouanne M, Thalmann GN, Veskimäe E, et al. European Association of Urology Guidelines on Muscle-invasive and Metastatic Bladder Cancer: Summary of the 2020 Guidelines. Eur Urol. 2021; 79:82–104. https://doi.org/10.1016/j.eururo.2020.03.055 PMID:32360052

24. Mosele F, Remon J, Mateo J, Westphalen CB, Barlesi F, Lolkema MP, Normanno N, Scarpa A, Robson M, Meric-Bernstam F, Wagle N, Stenzinger A, Bonastre J, et al. Recommendations for the use of next-generation sequencing (NGS) for patients with metastatic cancers: a report from the ESMO Precision Medicine Working Group. Ann Oncol. 2020; 31:1491–505. https://doi.org/10.1016/j.annonc.2020.07.014 PMID:32853681

25. Nishikura K. Functions and regulation of RNA editing by ADAR deaminases. Annu Rev Biochem. 2010; 79:321–49. https://doi.org/10.1146/annurev-biochem-060208-105251 PMID:20192758

26. Ramírez-Moya J, Miliotis C, Baker AR, Gregory RI, Slack FJ, Santisteban P. An ADAR1-dependent RNA editing event in the cyclin-dependent kinase CDK13 promotes thyroid cancer hallmarks. Mol Cancer. 2021; 20:115. https://doi.org/10.1186/s12943-021-01401-y PMID:34496885

27. Ramírez-Moya J, Baker AR, Slack FJ, Santisteban P. ADAR1-mediated RNA editing is a novel oncogenic process in thyroid cancer and regulates miR-200 activity. Oncogene. 2020; 39:3738–53. https://doi.org/10.1038/s41388-020-1248-x PMID:32157211

28. Li Z, Huang Y, Xu Y, Wang X, Wang H, Zhao S, Liu H, Yu G, Che X. Targeting ADAR1 suppresses progression and peritoneal metastasis of gastric cancer through Wnt/β-catenin pathway. J Cancer. 2021; 12:7334–48. https://doi.org/10.7150/jca.61031 PMID:35003354

29. Clara JA, Monge C, Yang Y, Takebe N. Targeting signalling pathways and the immune microenvironment of cancer stem cells - a clinical update. Nat Rev Clin Oncol. 2020; 17:204–32. https://doi.org/10.1038/s41571-019-0293-2 PMID:31792354

30. Ringlander J, Fingal J, Kann H, Prakash K, Rydell G, Andersson M, Martner A, Lindh M, Horal P, Hellstrand K, Kann M. Impact of ADAR-induced editing of minor viral RNA populations on replication and transmission of SARS-CoV-2. Proc Natl Acad Sci U S A. 2022; 119:e2112663119. https://doi.org/10.1073/pnas.2112663119 PMID:35064076

31. Baharom F, Ramirez-Valdez RA, Khalilnezhad A, Khalilnezhad S, Dillon M, Hermans D, Fussell S, Tobin KKS, Dutertre CA, Lynn GM, Müller S, Ginhoux F, Ishizuka AS, Seder RA. Systemic vaccination induces $CD8^+$ T cells and remodels the tumor microenvironment. Cell. 2022; 185:4317–32.e15. https://doi.org/10.1016/j.cell.2022.10.006 PMID:36302380

32. Dieu-Nosjean MC, Giraldo NA, Kaplon H, Germain C, Fridman WH, Sautès-Fridman C. Tertiary lymphoid structures, drivers of the anti-tumor responses in human cancers. Immunol Rev. 2016; 271:260–75. https://doi.org/10.1111/imr.12405 PMID:27088920

33. Wiede F, Lu KH, Du X, Liang S, Hochheiser K, Dodd GT, Goh PK, Kearney C, Meyran D, Beavis PA, Henderson MA, Park SL, Waithman J, et al. PTPN2 phosphatase deletion in T cells promotes anti-tumour immunity and CAR T-cell efficacy in solid tumours. EMBO J. 2020; 39:e103637. https://doi.org/10.15252/embj.2019103637 PMID:31803974

34. Margolis N, Moalem H, Meirson T, Galore-Haskel G, Markovits E, Baruch EN, Vizel B, Yeffet A, Kanterman-Rifman J, Debby A, Besser MJ, Schachter J, Markel G. Adenosine-Deaminase-Acting-on-RNA-1 Facilitates T-cell Migration toward Human Melanoma Cells. Cancer Immunol Res. 2022; 10:1127–40. https://doi.org/10.1158/2326-6066.CIR-21-0643 PMID:35731225

35. Zhao Y, Zheng X, Li M, Zhao J, Wang X, Zhu H. ADAR1 improved Treg cell function through the miR-21b/Foxp3 axis and inhibits the progression of acute graft-versus-host disease after allogeneic hematopoietic stem cell transplantation. Int Immunopharmacol. 2023; 115:109620. https://doi.org/10.1016/j.intimp.2022.109620 PMID:36577155

36. Johnson DB, Nebhan CA, Moslehi JJ, Balko JM. Immune-checkpoint inhibitors: long-term implications of toxicity. Nat Rev Clin Oncol. 2022; 19:254–67. https://doi.org/10.1038/s41571-022-00600-w PMID:35082367

37. Yamamoto H, Imai K. Microsatellite instability: an update. Arch Toxicol. 2015; 89:899–921. https://doi.org/10.1007/s00204-015-1474-0 PMID:25701956

SUPPLEMENTARY MATERIALS

Supplementary Figures

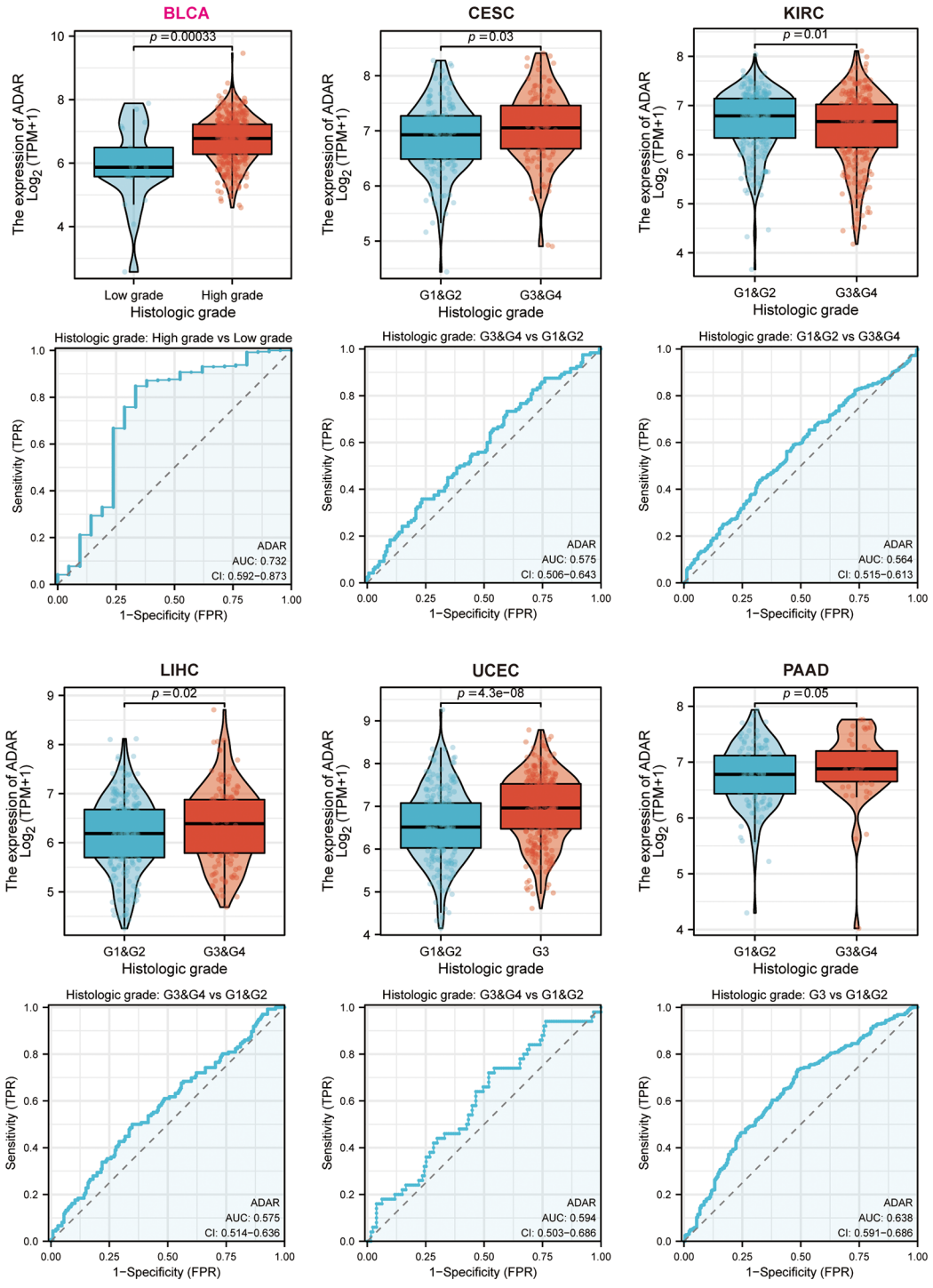

Supplementary Figure 1. ADAR expression was positively correlated with higher pathological grade in BLCA, CESC, LIHC, UCEC, and PAAD.

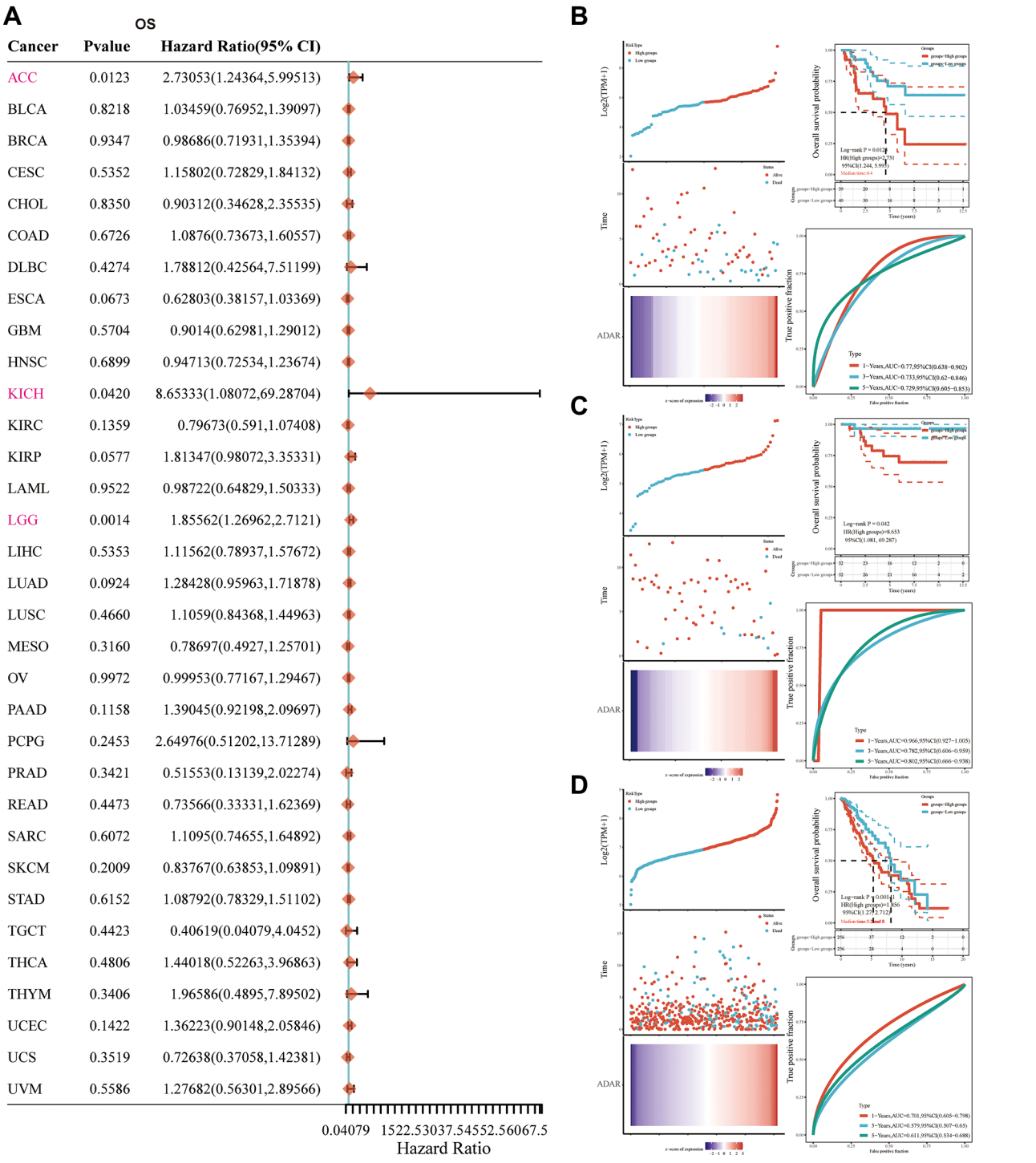

Supplementary Figure 2. ADAR expression with OS. (**A**) ADAR expression was associated with poor OS in ACC (HR = 2.73053, *P* = 0.0123), KIRP (HR = 8.65333, *P* = 0.0420), and LGG (HR = 1.85562, *P* = 0.0014). (**B**–**D**) Risk profiles and survival analyses of ADAR. High AUC values indicate high reliability of the prediction.

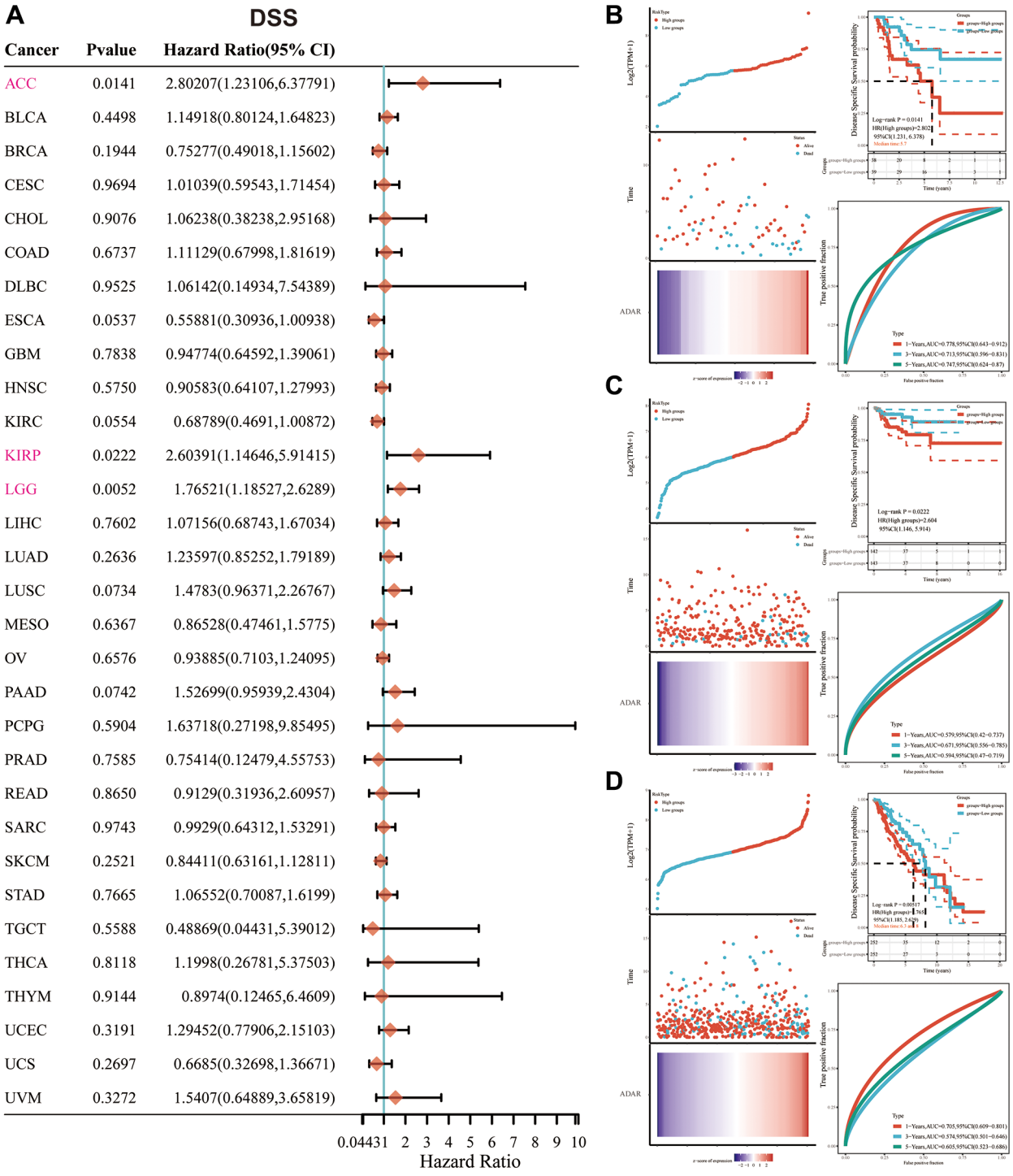

Supplementary Figure 3. ADAR expression with DSS. (**A**) ADAR was significantly associated with poor DSS in ACC (HR = 2.80207, *P* = 0.0141), KIRP (HR = 2.60391, *P* = 0.0222), and LGG (HR = 1.76521, *P* = 0.0052). (**B**–**D**) Risk profiles and survival analyses of ADAR. High AUC values indicate high reliability of the prediction.

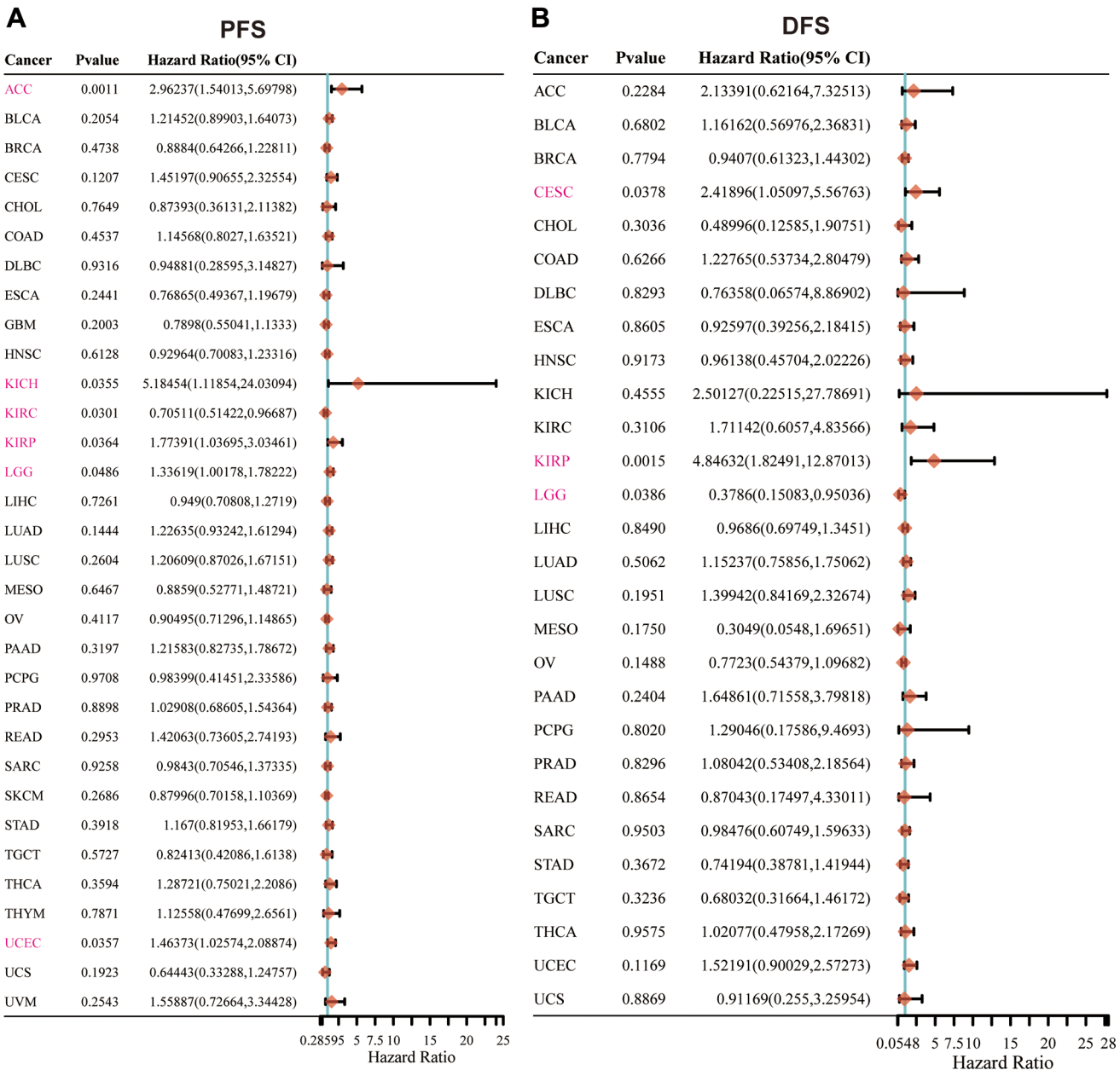

Supplementary Figure 4. Cox risk regression of ADAR in pan-cancer. (**A**, **B**) High ADAR expression predicted poor DFS in CESC (HR = 2.41896, *P* = 0.0378) and KIRP (HR = 4.84632, *P* = 0.0015), but was positively associated with better DFS in LGG (HR = 0.3786, *P* = 0.0386)

Supplementary Tables

Please browse Full Text version to see the data of Supplementary Table 3.

Supplementary Table 1. List of the top 100 ADAR-related genes from GEPIA2.0.

Gene symbol	Gene ID	PCC
ISG20L2	ENSG00000143319.16	0.75
YY1AP1	ENSG00000163374.19	0.74
SMG7	ENSG00000116698.20	0.72
EIF2AK2	ENSG00000055332.16	0.7
UBAP2L	ENSG00000143569.18	0.7
ATF6	ENSG00000118217.5	0.7
PIP5K1A	ENSG00000143398.19	0.7
CEP350	ENSG00000135837.15	0.69
UHMK1	ENSG00000152332.15	0.68
RAB3GAP2	ENSG00000118873.15	0.68
TAF5L	ENSG00000135801.9	0.67
COPA	ENSG00000122218.14	0.67
RPRD2	ENSG00000163125.15	0.67
GATAD2B	ENSG00000143614.7	0.67
RBM12	ENSG00000244462.7	0.67
WDR26	ENSG00000162923.14	0.67
ADNP	ENSG00000101126.15	0.67
TROVE2	ENSG00000116747.12	0.67
EXOC8	ENSG00000116903.7	0.67
HNRNPU	ENSG00000153187.16	0.66
AHCTF1	ENSG00000153207.14	0.66
UBE2Q1	ENSG00000160714.9	0.66
DIEXF	ENSG00000117597.17	0.66
ARNT	ENSG00000143437.20	0.66
SPRTN	ENSG00000010072.15	0.66
RBM12B	ENSG00000183808.11	0.65
ACBD3	ENSG00000182827.8	0.65
ARID4B	ENSG00000054267.20	0.65
RBBP5	ENSG00000117222.13	0.65
TRIP12	ENSG00000153827.13	0.65
PRRC2C	ENSG00000117523.15	0.65
BLZF1	ENSG00000117475.13	0.64
ASH1L	ENSG00000116539.10	0.64
SDE2	ENSG00000143751.9	0.64
POLR3C	ENSG00000186141.8	0.64
SP3	ENSG00000172845.13	0.64
TPM3	ENSG00000143549.19	0.64
URB2	ENSG00000135763.9	0.64
SCYL3	ENSG00000000457.13	0.64
HEATR1	ENSG00000119285.10	0.64
GOSR1	ENSG00000108587.14	0.63
POGK	ENSG00000143157.11	0.63
ETV3	ENSG00000117036.11	0.63
DTX3L	ENSG00000163840.9	0.63
USP37	ENSG00000135913.10	0.63
DEDD	ENSG00000158796.16	0.63
BROX	ENSG00000162819.11	0.63
BCLAF1	ENSG00000029363.15	0.63
THRAP3	ENSG00000054118.13	0.63
TRMT1L	ENSG00000121486.11	0.63

ANGEL2	ENSG00000174606.12	0.63
DDX46	ENSG00000145833.15	0.62
ZNFX1	ENSG00000124201.14	0.62
UHRF1BP1	ENSG00000065060.16	0.62
NSD1	ENSG00000165671.18	0.62
PRUNE	ENSG00000143363.15	0.62
TSNAX	ENSG00000116918.13	0.62
SNX27	ENSG00000143376.12	0.62
ZNF669	ENSG00000188295.14	0.62
ZMYM4	ENSG00000146463.11	0.62
ZNF281	ENSG00000162702.7	0.62
OTUD7B	ENSG00000264522.5	0.62
ZNF623	ENSG00000183309.11	0.62
NUP153	ENSG00000124789.11	0.62
FAM20B	ENSG00000116199.11	0.62
HNRNPK	ENSG00000165119.18	0.61
UBN1	ENSG00000118900.14	0.61
GTF3C4	ENSG00000125484.11	0.61
CNOT6	ENSG00000113300.11	0.61
RBM27	ENSG00000091009.7	0.61
ZSCAN29	ENSG00000140265.12	0.61
METTL14	ENSG00000145388.14	0.61
SENP1	ENSG00000079387.13	0.61
CELF1	ENSG00000149187.17	0.61
RFX5	ENSG00000143390.17	0.61
IARS2	ENSG00000067704.9	0.61
GPR89A	ENSG00000117262.18	0.61
CREB1	ENSG00000118260.14	0.61
WAC	ENSG00000095787.21	0.61
CACUL1	ENSG00000151893.14	0.61
SLC25A44	ENSG00000160785.13	0.6
PUM2	ENSG00000055917.15	0.6
CDC73	ENSG00000134371.9	0.6
POGZ	ENSG00000143442.21	0.6
ZBTB41	ENSG00000177888.7	0.6
PYGO2	ENSG00000163348.3	0.6
NUP133	ENSG00000069248.11	0.6
UBQLN4	ENSG00000160803.7	0.6
STX17	ENSG00000136874.10	0.6
YME1L1	ENSG00000136758.18	0.6
CSNK1G1	ENSG00000169118.15	0.6
7-Mar	ENSG00000136536.14	0.6
SIN3A	ENSG00000169375.15	0.6
KDM5B	ENSG00000117139.16	0.6
CDC42SE1	ENSG00000197622.12	0.6
CAPRIN1	ENSG00000135387.19	0.6
INTS7	ENSG00000143493.12	0.59
SMEK2	ENSG00000275052.4	0.59
FBXW2	ENSG00000119402.16	0.59
PGGT1B	ENSG00000164219.9	0.59

Supplementary Table 2. Correlation analysis between ADAR expression and immune cell clustering.

ID	Main specificity	Main function	#Genes	Annotation reliability
1	T-cells	Immune response	378	High
2	T-cells	T-cell receptor	243	Medium
3	Suprabasal keratinocytes	Cornification	185	High
4	Platelets	Platelet activation	157	High
5	Bronchus	Unknown function	208	Low
6	Late spermatids	Spermatogenesis	433	Medium
7	NK-cells	Immune response regulation	312	Medium
8	Oligodendrocytes	Myelin sheath organization	301	Medium
9	Neurons	Nervous system development	235	Medium
10	Neurons and Oligodendrocytes	Nervous system development	262	High
11	Non-specific	Transcription	188	Medium
12	Non-specific	Chromatin organization	249	Low
13	Hepatocytes	Oxidoreductase activity	177	High
14	Endometrium	Transcription regulation	304	Low
15	Smooth muscle cells	Muscle contraction	246	High
16	Non-specific	RNA binding	751	Low
17	Granulosa cells	Transcription regulation	353	Medium
18	Non-specific	Mixed function	294	Low
19	Macrophages	Innate immune response	247	High
20	Airway and Pancreas	Proteolysis	48	Medium
21	Serous glandular cells	Salivary secretion	134	Medium
22	Squamous epithelial cells	Keratinization	298	High
23	Langerhans cells	Immune response	91	Medium
24	Spermatids	Unknown function	117	Low
25	Schwann cells and Melanocytes	Mixed function	80	Low
26	Intestinal epithelial cells	Absorption	271	High
27	Skeletal myocytes	Muscle contraction	105	High
28	Cytotrophoblasts	Unknown function	227	Low
29	Hepatocytes	Metabolism	152	Medium
30	Breast	Lactation	82	High
31	Spermatocytes	Spermatogenesis	213	High
32	Neurons	Synaptic function	237	High
33	Macrophages	Degranulation	283	High
34	Plasma cells	Humoral immune response	86	High
35	Bipolar cells	Visual perception	159	High
36	Spermatids	Spermatogenesis	419	High
37	Neurons	Neuronal signaling	496	High
38	Neurons	Neuronal signaling	626	High
39	Non-specific	Translation	186	Medium
40	Plasma cells	Humoral immune response	409	Medium
41	Alveolar cells	Lung function	118	Medium
42	Spermatocytes and Spermatids	Spermatogenesis	353	Medium

43	Non-specific	Cell proliferation	263	Medium
44	Photoreceptor cells	Visual perception	359	High
45	Plasma cells	Humoral immune response	78	High
46	Granulocytes	Mast cell degranulation	60	Medium
47	Spermatogonia	Spermatogenesis	119	Medium
48	Plasmacytoid dendritic cells	Unknown function	134	Low
49	Early spermatids	Spermatogenesis	272	High
50	Enterocytes	Absorption	308	Medium
51	Late spermatids	Spermatogenesis	389	High
52	Endometrial stromal cells	ECM organization	116	Medium
53	Connective tissue cells	ECM organization	187	Medium
54	Extravillous trophoblasts	Unknown function	188	Medium
55	Endocrine cells	Hormone signaling	81	High
56	Ciliated cells	Cilium assembly	425	High
57	Early spermatids	Flagellum and Golgi organization	325	Medium
58	Gastric mucus-secreting cells	Digestion	45	High
59	Proximal enterocytes	Transmembrane transport	209	High
60	Proximal tubular cells	Absorption	361	High
61	Non-specific	Transcription	366	Low
62	B-cells	B-cell activation	166	High
63	Astrocytes	Nervous system maintenance	208	High
64	Non-specific	Transcription	655	Medium
65	Fibroblasts	ECM organization	292	High
66	Endothelial cells	Angiogenesis	468	Medium
67	Syncytiotrophoblasts	Pregnancy	153	Medium
68	Muller glia cells	Visual perception	142	High
69	Macrophages	Innate immune response	217	High
70	Basal prostatic cells	Lipid metabolism	167	Medium
71	Erythroid cells	Oxygen transport	140	High
72	Smooth muscle cells	ECM organization	208	High
73	Prostatic glandular cells	Transcription	109	High
74	Pancreatic cells	Mixed function	331	Low
75	Myeloid cells	Innate immune response	390	Medium
76	Spermatocytes and Spermatogonia	Spermatogenesis	164	High
77	Cardiomyocytes	Muscle contraction	404	High

Supplementary Table 3. Differentially expressed genes between the ADAR high-expression group and the ADAR low-expression group.